

Trade and the Competition for Transport:

How (a Lack of) Competition in the Transportation Industry Affects Regional Trade Outcomes*

C Adam Pfander
University of Colorado, Boulder
Contact: charles.pfander@colorado.edu

DRAFT: PRELIMINARY AND INCOMPLETE. DO NOT CITE
WITHOUT AUTHOR'S PERMISSION.

Updated: October 24, 2023
Most recent version available [here](#).

Abstract

This paper seeks to understand how market structure for freight transportation affects domestic trade outcomes. I modify a standard Ricardian trade model to incorporate imperfectly-collusive transporters spanning multiple modes. Estimating the model's fundamentals reveals the expected per-mile iceberg trade cost for specific modes, the correlation of trade costs across disparate markets, and the ferocity of competition for freight transportation along individual segments of the domestic transit network. Calibrating the model to domestic trade flows, I find that: i) current losses due to non-competitive pricing are substantial, amounting to roughly 5% of baseline welfare; ii) the exercise of freight market power has an outsize impact on exports; iii) these impacts are concentrated in rural areas throughout the Southeast and Mountain West, as well as small urban areas in the Midwest and Gulf states; iv) exercise of freight market power exacerbates the impact of mode-specific shocks; and v) non-competitive freight pricing does little to attenuate international trade shocks, due to the concentration of freight market power away from international gates.

*This paper benefited tremendously from the feedback of Taylor Jaworski, Wolfgang Keller, Richard Mansfield, and Scott Savage. I also thank the members of the trade, IO, and grad-student brownbags at the University of Colorado, Boulder for their continued input. A special thanks goes to the participants of the graduate student workshop at the Western Economic Conference for their invaluable feedback. I also owe a particular debt of gratitude to my advisor, Jeronimo Carballo, for his constant guidance, support, and patience. I also give thanks to the team behind the R Project for statistical computing (R Core Team, 2022), as well as the authors of the following packages: dplyr (Wickham et al., 2022), magrittr (Bache and Wickham, 2022), data.table (Dowle and Srinivasan, 2023), doParallel (Microsoft and Weston, 2022a), foreach (Microsoft and Weston, 2022b), fixest (Bergé, 2018), DescTools (Andri et mult. al., 2022), stringr (Wickham, 2022), ggmap (Kahle and Wickham, 2013), dqrng (Stubner, 2021), and RPostgres (Wickham et al., 2023). I also acknowledge the creators of and contributors to PostgreSQL.

All remaining errors are my own.

1 Introduction

Transportation is central to trade: how a good moves from its origin to its destination largely dictates its final price. Yet conventional trade models abstract away from the freight-service industry by assuming purely exogenous transport costs.¹ Recognizing this insufficiency, a raft of recent papers have sought to incorporate more realistic transportation sectors into canonical trade models. Specifically, these recent works model route-choice (Allen and Arkolakis, 2022; Allen and Arkolakis, 2014), mode-choice (Fuchs and Wong, 2023), and port-choice (Brancaccio et al., 2020) to generate trade costs as a function of existing infrastructure. Sorely missing from this line of inquiry, however, is a comprehensive analysis of freight transporters' strategic price-setting behavior.

This paper seeks to understand the role of the freight industry in setting domestic trade outcomes. To build upon recent work in this area, I generate a comprehensive model of the transporter's pricing decision; importantly, I utilize long-standing methods from the industrial organization literature to empirically evaluate the ferocity of freight market competition in distinct locations across the mainland United States. Moreover, I incorporate the route-choice, mode-choice, and port-choice problems mentioned previously, such that trade costs reflect not only competition for freight services, but available infrastructure as well. This discrete choice framework has the added benefit of incorporating imperfect substitution across origins, modes, and even distinct routes. The combination of these disparate modeling choices provides a comprehensive view of how the transportation sector influences domestic trade outcomes. I further relax the strict independence assumptions which pervade conventional trade models, and allow correlation of trade costs across competing origins and routes; this generalization permits more realistic substitution patterns across competing modes and trade routes.² The model provides a straightforward framework to estimate: i) the state of competition among freight carriers within individual cities and modes throughout the mainland US; ii) expected trade costs along all major trade routes in the Lower-48; and iii) the correlation of these trade costs among distinct routes serving the same market. Beyond a descrip-

¹This strict exogeneity assumption stems from Samuelson (1954), who first proposed an exogenous iceberg trade cost formulation in order to generate a tractable expression of trade flows. While convenient, this assumption is undoubtedly an oversimplification

²The assumption of perfectly independent trade costs, made originally for analytical convenience (Eaton and Kortum, 2002), implies unrealistic substitution patterns, and thus undermines the reliability of counterfactual simulations (Train et al., 1987). See Lind and Ramondo (2023) for a complete discussion of correlated trade costs in Ricardian models.

tive tool, the model is useful for policy evaluation; I run a series of counterfactual simulations to estimate how imperfect competition for transport services exacerbates and/or mitigates the welfare impacts of a domestic transport shock as well as an international trade shock. The model thus provides a powerful framework to estimate the impact of imperfect competition for freight transport on the U.S. economy.

Several trade papers relate market structure in the transportation industry to trade outcomes (Brancaccio et al., 2020; Atkin and Donaldson, 2015). None, however, models the competition within and across competition modes, and within distinct geographies. I build upon longstanding insights from empirical IO to summarize the ferocity of freight-market competition in distinct locations across the U.S. via a handful of parameters (Bresnahan, 1982; Miller and Weinberg, 2017); these conduct parameters, in turn, inform freight markups along individual trade routes throughout the mainland U.S.. The power of this approach is that it does not assume a particular solution concept (e.g. Bertrand, Cournot, etc.). Rather, the theory permits a continuum of competitive outcomes; the prevailing equilibrium for an individual location is identified empirically. Moreover, this competition parameterization nests neatly within an otherwise standard iceberg trade cost formulation, thus retaining a simple gravity expression for trade flows. In other words, my model flexibly captures the competitive landscape for freight services within individual modes throughout the mainland US while maintaining the empirically tractable log-linear expression of trade flows that is the hallmark of conventional gravity models.

The model also reflects the multifaceted and supremely dense nature of the US transit network. Between every origin and destination pairing, I allow not only a comprehensive set of modes,³ but also multiple routes along each mode. This highly detailed choice structure is appealing first for its realism – instead of assuming a unique least-cost route between any two locations,⁴ my model permits trade flows among alternate paths; these competing, parallel flows stem from unobserved, idiosyncratic efficiencies among transporters. Second, as demonstrated by Allen and Arkolakis (2022) as well as Fuchs and Wong (2023), modelling the transporter’s route-choice problem allows

³Specifically, I analyse domestic freight movements via road, rail, inland and ocean waterways, air, as well as multi-modal movements. I exclude freight via pipeline, as it serves only a narrow subset of goods (i.e. crude oil, natural gas, and other petroleum products). The set of modes considered for any one origin-destination combination is determined by the presence of the relevant infrastructure. That is, I do not allow movements via – for example – water if no navigable waterway unites the two locations; the same logic applies to all modes. See section 3 for detail.

⁴Such a uniqueness assumption is usually made due to data constraints and/or for analytical convenience. See, e.g., Allen and Arkolakis (2014), Donaldson and Hornbeck (2016), and Donaldson (2018), among others.

me to express trade costs (and hence, trade flows) as a function of available infrastructure; the upshot of this approach in my model is that the estimated conduct parameters reflect the density of the network.⁵ Finally, this approach easily lends itself to a nested-logit formulation of trade shares (McFadden, 1984), which in turn offers a convenient and straightforward framework to evaluate the correlation of trade costs across competing routes serving the same destination.⁶

The model offers highly-granular, route-level insights; it is therefore notable that I estimate these fundamentals using exclusively public data. To elaborate, I populate potential trade routes using detailed topographic information on the domestic transportation network from the National Transportation Atlas Databases (NTAD); I retrieve domestic trade flows in 2017 from the Freight Analysis Framework version 5 (FAF5). Both of these datasets are publicly-available from the Bureau of Transportation Statistics (BTS). However, the FAF5 data are aggregated by origin, destination, and mode; it does not provide route-level trade flows, which are necessary for estimation. I therefore rely on an expectation-maximization (EM) process – a well-known simulated method of moments strategy from the computer science literature, which has been used to some extent in the field of economics (e.g. Bonadio, 2021). No existing paper provides such a comprehensive and detailed view of the transportation sector using only public information.⁷

The model yields five, principal insights. First, I find that current losses due to non-competitive freight pricing are substantial, equal approximately 5% of current welfare. The lion's share of these losses stem from the Road, a finding supported by anecdotal evidence of pervasive supply chain bottlenecks – hence, market power – throughout the trucking industry. Second, the exercise of freight market power has an outsize influence on exports; imposing perfectly competitive freight pricing may increase exports by as much as 20% but imports only 7%. This result suggests that

⁵Why should density matter for the transporters' pricing game? Routes serving the same origin-destination pairing are close substitutes. Sparse portions of the network thus imply a relative absence of close substitutes (or more precisely, the substitutes are less cost-competitive), which suggests greater opportunity to exploit market power. Indeed, I find that current welfare losses due to non-competitive freight pricing are greatest among rural areas along relatively sparse portions of the network.

⁶Lind and Ramondo (2023) propose an Eaton and Kortum (EK) trade model with correlation of efficiencies across countries. They demonstrate that the conventional independence assumption is nontrivial, leading to vastly different welfare estimates than found using their correlation structure. I build upon their approach by allowing correlation of both production and transport efficiencies; these correlations, in turn, inform markups (see Section 2 for detail).

⁷Other papers estimate detailed trade costs using confidential data. Most recently, Fuchs and Wong (2023) utilize the confidential waybill sample to estimate the impact of rail (as well as port) congestion throughout the domestic transport network; Brancaccio et al. (2020) estimate bargained freight rates using proprietary transaction data from Clarkson's Research. Others utilize public data, but narrow their focus to a subset of modes – for example, Allen and Arkolakis (2022) focus on roads; Donaldson (2018) focus on rails; Ducruet et al. (2020) focus on shipping networks.

managing non-competitive freight pricing offers a new lever to influence the U.S. trade deficit, which is of substantial interest to policy makers. Third, I document significant geographic heterogeneity in the exercise of freight market power. Potential gains from elimination of freight market power are concentrated in rural areas in the Southeast and Mountain West, as well as small urban areas throughout the Midwest and along the Gulf of Mexico; major international gates stand the least to gain from a perfectly-competitive freight market. Shutting down a single mode sparks dramatic welfare losses; the exercise of market power exacerbates these losses.⁸ This result underscores that, in the event of national, mode-specific shocks, we should expect a meaningful pricing response from competing modes. Finally, due to the concentration of freight market power away from international gates, I report near-perfect pass-through of international trade shocks; inland areas along sparse portions of the network suffer greatest.

This paper contributes to a growing body of trade papers, which explore the impact of freight transportation and infrastructure on trade outcomes. Recent papers along this line of inquiry have analysed the welfare effects of road and/or port congestion (Allen and Arkolakis, 2022; Bonadio, 2021; Fuchs and Wong, 2023), containerization (Coşar and Demir, 2018), and most popularly, network development/expansion (Jaworski et al., 2022; Ganapati et al., 2021; Donaldson, 2018; Ducruet et al., 2020; Donaldson and Hornbeck, 2016; Faber, 2014). However, all of these papers analyze only one or two modalities – e.g. roads, rail, or ports/ships. In contrast, I model all available modes simultaneously. Capturing the multi-faceted nature of the US transit network is important when studying the transporter’s pricing decision, as competition weighs both within and across modes. Said differently, the consumer likely does not care *how* a good got to its destination, only that it arrived and its cheaper than all (quality-adjusted) alternatives. Thus, to stay cost-competitive, modes must compete with one another.⁹ My primary contribution to this literature is to model competition among freight service providers, capturing price pressures both within and across modes.

The importance of multi-modal transport to domestic trade outcomes is highlighted in the

⁸The analysis that yields this result is inspired by the narrowly-avoided rail strike of 2022, which would have halted all rail traffic and the vast majority of multi-modal movements.

⁹Throughout the latter half of the 20th Century, domestic freight in the US was dominated by trucking. However, recent technological improvements, which facilitate near-seamless transshipment, have given new life to competing modes; multi-modal movements are now the second-most popular form of transit domestically (Bureau of Transportation Statistics and Federal Highway Administration, U.S. DOT, 2022).

parallel work by Fuchs and Wong (2023). In this important paper, the authors build upon a highly-tractable model of traffic flows (Allen and Arkolakis, 2022), to encompass multiple modes and costly transshipment. The upshot of this approach is that the authors may quantify how congestion along any one mode spills into the wider network; importantly, they identify key bottlenecks throughout the domestic transit network and estimate how even slight investments at these choke points create substantial welfare gains throughout the nation. This paper underscores the importance of multi-modal shipping to domestic trade outcomes; however, the authors do not consider the role of competition in setting freight rates. I build upon their framework by incorporating the transporter's strategic pricing decision.

The present paper is most closely related to Brancaccio et al. (2020). In this work, the authors model the transport market with a matching function; freight rates are set via Nash bargaining. This paper is the first to model how transporters' strategic behavior impacts trade flows; however, their focus is solely on ships in the international freight market. In contrast, I focus on the multi-modal domestic transport network. Further, their matching function approach – which they utilize to explain ships' ballasting choices – is governed by one, global bargaining parameter. In contrast, I evaluate the state of market power within distinct markets throughout the mainland U.S.. My model thus offers a highly-granular assessment of how competition for transport within individual locations affects trade locally, and nationally.

The rest of the paper is organized as follows. Section 2 develops my theoretical model, distinguishing between transport demand – equilibrium trade flows – and supply – a model of transporter's optimal pricing rule. Section 3 details my strategy for estimating the model fundamentals; it presents my data sources and expounds upon the EM algorithm, which exploits the structure of the model to estimate route-level trade costs from aggregated data. Section 4 discusses my estimated parameters, model validation exercises, and robustness checks. Section 5 details my counterfactual simulations. Section 6 concludes.

2 Theoretical Model

I develop a Ricardian trade model, in which each origin-destination combination is served by a representative freight transporter. These intermediaries span multiple modes, and may pick among

a selection of routes per mode. I emphasize that transporters need not take the shortest path, but may elect more circuitous routes if they appear more profitable due to unobserved, exogenous costs. Further, transporters set markups endogenously to maximize profits; the key inputs into the transporter's problem include demand for freight transport into a domestic market, the costs incurred en-route, and the ferocity of freight-market competition along a particular route. Regarding competition among transporters: I do not take a stand a priori on a particular solution to the transporter's pricing game, but adapt Bresnahan (1982)'s method to develop a pricing rule that admits a wide array of competitive outcomes, including the extremes of perfect competition and perfect monopoly. I now describe the model in detail.

2.1 Transportation Demand: Equilibrium Trade Flows

I begin with the familiar Eaton and Kortum (2002) framework, henceforth termed “EK”. Trade in a unit-mass of goods Ω occurs amongst a discrete, finite set of locations \mathcal{S} ; let $i, j \in \mathcal{S}$ denote the ultimate origin, destination. I further distinguish between domestic locations $\mathcal{S}^d \subset \mathcal{S}$ and foreign locations $\mathcal{S}^f \subset \mathcal{S}$, noting that $\mathcal{S}^d \cap \mathcal{S}^f = \emptyset$. Let $e, x \in \mathcal{S}^d$ denote a shipment's port of entry, exit into/out of the mainland U.S.. For domestic origins (destinations), the port of entry (exit) is equivalent to the final origin (destination).¹⁰

All domestic locations lie on a graph and are connected by a set of edges. A route between a domestic origin and destination, $e, x \in \mathcal{S}^d$, comprises a set of edges that form an unbroken path between e and x . Routes need not be direct, but I do require them to be simple – that is, a route may take a circuitous path on its way from e to x , but no repeating edges.¹¹ Let \mathcal{R}_{ex} denote the set of all routes linking e to x . I may further decompose this set by mode of transport. Let $\mathcal{M} = \{\text{Road, Rail, Water, Air, Multi-modal}\}$ denote the set of available modes and let $\mathcal{R}_{ex}^m \subseteq \mathcal{R}_{ex}$ denote the subset of routes between e and x via mode $m \in \mathcal{M}$.¹² Figure 2 provides an illustrative example of the domestic transit network.

Traversing the network is costly. Let $\tau_{ir(e,x,m)j}$ denote the cost of traversing route $r \in \mathcal{R}_{ex}^m$ ¹³

¹⁰Explicitly, $i \in \mathcal{S}^d \iff i = e$ and $j \in \mathcal{S}^d \iff x = j$.

¹¹Note also that routes are direction-dependent: the set of edges forming a path from e to x is distinct from the same path moving from x to e , though their observable characteristics are identical.

¹²It is important to note that the set of modes is exhaustive, such that $\mathcal{R}_{ex} = \cup_{m \in \mathcal{M}} \mathcal{R}_{ex}^m \forall e, x \in \mathcal{S}^d$. Additionally, with the exception of Multi-modal transport, these paths are mutually exclusive, $\mathcal{R}_{ex}^m \cap \mathcal{R}_{ex}^{m'} = \emptyset \forall m, m' \in \mathcal{M} \setminus \{\text{Multi-Modal}\}, m \neq m'$, and $\forall i, j \in \mathcal{S}$.

¹³Note that knowledge of the route implies knowledge of the domestic origin e , destination x , and mode m . For

between i and j ; these transit costs take the standard iceberg formulation. I further assume that each origin enjoys a uniform input cost c_i and employs constant returns to scale technology. Finally, I impose perfect competition in the goods market, such that the price of good ω , produced in i , consumed in j , and taking route r via mode m between the two is given by

$$p_{irj}(\omega) = \frac{c_i \tau_{ijr} \mu_{irj}}{\epsilon_{irj}(\omega)}, \quad (1)$$

where μ_{irj} is an endogenous markup set by the transporter, and $\epsilon_{ijr}(\omega)$ is a composite production and transportation efficiency, which I will elaborate shortly. But first, I want to highlight that prices vary not only by their origin, but by the route taken en route to market. Thanks to perfect competition in the market for tradeable goods, the price paid by the consumer is the cheapest available alternative. That is:

$$p_j(\omega) = \min_{i \in \mathcal{S}} \left\{ \min_{e, x \in \mathcal{S}^d} \left\{ \min_{m \in \mathcal{M}} \left\{ \min_{r \in \mathcal{R}_{ex}^m} p_{ijr}(\omega) \right\} \right\} \right\}.$$

As in the traditional EK model, I rely on a probabilistic representation of composite efficiencies to relate trade flows across locations and routes to a handful of easy-to-interpret parameters. Unlike the standard model, I follow McFadden (1984) to allow correlation of efficiencies within distinct destinations, origins, ports of entry/exit, and modes. Explicitly, the joint distribution function for the vector of log efficiencies is given by:

$$F_j \begin{pmatrix} \ln \epsilon(\omega)_1 \\ \ln \epsilon(\omega)_2 \\ \vdots \end{pmatrix} = \exp \left(- \sum_{i \in \mathcal{S}} \left(\sum_{e, x \in \mathcal{S}^d} \left(\sum_{m \in \mathcal{M}} \left(\sum_{r \in \mathcal{R}_{ex}^m} \exp \left(\frac{-\ln A_i - \theta \ln \epsilon_r(\omega)}{\varphi \rho \zeta} \right) \right)^\varphi \right)^\rho \right)^\zeta \right). \quad (2)$$

In words, I assume a generalized extreme value distribution with location parameter A_i and scale parameter θ . The parameters φ, ρ , and $\zeta \in (0, 1]$ respectively govern the correlation of efficiencies within distinct nests—respectively, modes, ports of entry/exit, and origins. A value of 1 implies no correlation among these efficiencies within a given nest, while 0 implies perfect correlation. Due to this correlation structure, the interpretation of parameters is somewhat altered from the original EK model. A_i governs absolute advantage, while φ, ρ , and ζ , along with θ jointly determine the prevalence of comparative advantage.¹⁴ Details of the nesting structure are presented in Figure 1.

ease of exposition, I will omit the extraneous subscripts where expedient.

¹⁴See Lind and Ramondo (2023) for a complete discussion of how allowing correlation of efficiencies changes the interpretation of the EK model.

Equation (2) is a generalization of the hallmark Fréchet assumption from the canonical Eaton and Kortum model. This formulation is attractive for two, key reasons. First, this logit demand formulation treats transport along different routes as differentiated services. Hence, trade from competing origins, modes, and even different routes serving the same market, function as imperfect substitutes. Second, the nesting structure dispenses with the assumption that efficiency shocks are independent across locations; rather, the model permits a highly flexible correlation structure across destinations, origins, ports of entry/exit, and modes. This correlation structure relaxes the independence of irrelevant alternatives (IIA) assumption inherent in the standard logit model, which implies strict and often unrealistic substitution patterns. In this model, I require IIA to hold within, but not across nests.¹⁵

I assume the following functional form for trade costs:

$$\tau_{ir(e,x,m)j} = \exp \left(\underbrace{\mu_{irj}}_{\text{markup}} + \underbrace{\kappa_r}_{\text{deterministic costs}} + \underbrace{u_{irj}}_{\text{unobserved quality}} + \underbrace{\eta_{ie} + \nu_{xj}}_{\text{international trade cost}} + \underbrace{\alpha_{iem}}_{\text{first mile}} + \underbrace{\gamma_{xmj}}_{\text{final mile}} \right) \quad (3)$$

I now detail each component. Transporters set μ_{irj} to maximize profit, based on the demand and competition for transport services in geographically distinct markets (see Section 2.2 for detail). The deterministic component, κ_r , reflects the costs incurred per-mile while moving along a route – practically, this includes the cost of fuel, labor, and maintenance, and is taken as exogenous. The parameter u_{irj} is a structural error term and reflects unobserved route quality. Following Berry (1994), I assume $u_r \sim N(0, v)$, and is drawn independently across routes. The parameters η_{ie} and ν_{xj} capture costs incurred along the international leg of the journey (if any). Explicitly, η_{ie} presents the cost of travelling from an international origin i to a domestic port of entry e , while ν_{xj} is the cost of travelling from a domestic port of exit x to a foreign destination j . Finally, the parameters α_{iem} and γ_{xmj} capture a wide array of otherwise unobserved location-by-mode-specific costs. These include the cost of entering/exiting a domestic location via mode m , and reflect, e.g., port, yard, and/or inner-city congestion. These parameters also capture stand-alone, mode-specific costs, such as loading times, product composition, network-wide congestion, and/or reliability.

¹⁵To illustrate the potential pitfalls of IIA, consider the following, stylized example. Imagine that a transporter introduces a new rail route between an arbitrary origin and destination. Naturally, this new route will siphon traffic away from existing trade routes. IIA requires that the new route will draw from other routes in proportion to their trade shares, such that the ratio of trade shares among existing routes remains constant. However, it seems far more likely that the new rail line will disproportionately draw trade away from other rail routes, and have less of an impact on trade via other modes. The nested structure of my model captures this more realistic substitution pattern.

The distributional assumption on composite efficiencies, coupled with perfect competition in the market for tradeable goods, yields a nested logit¹⁶ formulation for trade shares within each market j :¹⁷

$$\pi_{r|iexmj} = \exp \left(-\theta[\mu_{irj} + \kappa_r + u_{irj}] / (\varphi\rho\zeta) - J_{iexmj} \right) \quad (4)$$

$$\pi_{m|ieej} = \exp \left(-\theta[\alpha_{iem} + \gamma_{mxj}] / (\rho\zeta) + \varphi J_{ieej} - V_{ex} \right) \quad (5)$$

$$\pi_{ex|ij} = \exp \left(-\theta[\eta_{ie} + \nu_{xj}] / \zeta + \rho V_{ieej} - I_{ij} \right) \quad (6)$$

$$\pi_{i|j} = \exp \left(-\ln A_i - \theta \ln c_i + \zeta I_{ij} - Q_j \right) \quad (7)$$

where

$$J_{ieej} = \ln \sum_{r \in \mathcal{R}_ex^m} \exp \left(-\theta[\mu_{irj} + \kappa_r + u_{irj}] / (\varphi\rho\zeta) \right) \quad (8)$$

$$V_{ieej} = \ln \sum_{m \in \mathcal{M}} \exp \left(-\theta[\alpha_{iem} + \gamma_{jxm}] / (\rho\zeta) + \varphi J_{ieej} \right) \quad (9)$$

$$I_{ij} = \ln \sum_{e,x \in \mathcal{S}^d} \exp \left(-\theta[\eta_{ie} + \nu_{xj}] / \zeta + \rho V_{ex} \right) \quad (10)$$

$$Q_j = \ln \sum_{i \in \mathcal{S}} \exp \left(-\ln A_i - \theta \ln c_i + \zeta I_{ij} \right). \quad (11)$$

Combining these conditional probabilities yields the following log-linear expression for the trade share along any one route:

$$\begin{aligned} \pi_{ir(e,x,m)|j} &= \pi_{r|ieej} \pi_{m|ieej} \pi_{ex|ij} \pi_{i|j} \\ &= \exp \left(-\ln A_i - \theta \left[\ln c_i + (\mu_{irj} + \kappa_r + u_{irj}) / (\varphi\rho\zeta) + (\alpha_{iem} + \gamma_{jxm}) / (\rho\zeta) + (\eta_{ie} + \nu_{xj}) / \zeta \right] \right. \\ &\quad \left. - (1 - \varphi) J_{ieej} - (1 - \rho) V_{ieej} - (1 - \zeta) I_{ij} - Q_j \right). \end{aligned}$$

Some straightforward (though tedious) algebra yields (see Appendix A.1 for detail):

$$\begin{aligned} \pi_{ir(e,x,m)|j} &= \exp \left(-\ln A_i - \theta \left[\ln c_i + \mu_{irj} + \kappa_r + u_{irj} + \alpha_{iem} + \gamma_{jxm} + \eta_{ie} + \nu_{xj} \right] \right. \\ &\quad \left. + (1 - \varphi\rho\zeta) \ln \pi_{r|ieej} + (1 - \rho\zeta) \ln \pi_{m|ieej} + (1 - \zeta) \ln \pi_{ex|ij} - Q_j \right). \quad (12) \end{aligned}$$

Finally, consumers enjoy CES utility with elasticity parameter $\sigma \in (1, \theta + 1]$. Explicitly, con-

¹⁶Note that if any one correlation parameter equals 1, then that nest effectively dissolves and is absorbed into the higher nest; if $\varphi = \rho = \zeta = 1$, the model collapses to a standard EK trade model with trade elasticity θ (McFadden, 1984; Eaton and Kortum, 2002).

¹⁷See Train et al., 1987 for detailed derivations.

sumers consume a quantity of each good, $q(\omega)$ to maximize $U = \left(\int_{\Omega} q(\omega)^{\frac{\sigma-1}{\sigma}} d\omega \right)^{\frac{\sigma}{\sigma-1}}$ subject to a budget constraint that aggregates to a trade balance condition. That is, the sum total value of imports must equal the sum total value of exports in location j . The assumption of CES utility implies a CES price index in location j (see Appendix A.2 for detail). Further, I adhere to the structure laid out in Eaton and Kortum (2002) and assume a Cobb-Douglas aggregate of input costs, with labor having a constant share β . These conditions yield expressions for input costs, prices, and wages:

$$c_i = w_i^\beta p_i^{1-\beta} \quad (13)$$

$$p_j = \Gamma \left(\frac{\theta + 1 - \sigma}{\theta} \right)^{\frac{1}{1-\sigma}} Q_j^{-\frac{1}{\theta}} \quad (14)$$

$$L_i w_i = \sum_{k \in \mathcal{S}} \sum_{e, x \in \mathcal{S}} \sum_{r \in \mathcal{R}_{ex}} \pi_{ir|k} L_k w_k \quad (15)$$

where w_i , L_i are the wage, population in location i , and Γ denotes the gamma function. Taken together, Equations (4) - (15) characterize a modified Ricardian model of trade, allowing for a multiplicity of trade routes between locations, imperfect modal substitution, and imperfect competition for freight transport services.

2.2 Transportation Supply: Setting Markups

Given appropriate data, estimating Equation (12) is straightforward. However, I do not observe costs or prices in the freight industry (see Section 3.1 for detail), meaning route-level markups μ_{irj} are unknown ex-ante. I thus impose additional structure on the transporter's pricing decision. The goal of this theoretical undertaking is to parameterize μ_{irj} such that: i) markups are a function of observable data; and ii) I do not assume a particular to the transporter's pricing game, but permit a wide array of potential equilibria, including the extremes of perfect competition and perfect monopoly. Luckily, long-standing insights from empirical IO provide such a framework (Bresnahan, 1982; Miller and Weinberg, 2017); I now detail the structure that yields this result.

A representative transporter of mode m servers an origin-destination pairing ij . Given the scale of the transporter's problem, it is convenient to characterize its total profit in matrix notation. Accordingly, define $\boldsymbol{\pi}_{imj}^\top = \begin{bmatrix} \pi_{ir_1|j} & \pi_{ir_2|j} & \dots \end{bmatrix}$, $\boldsymbol{\mu}_{imj}^\top = \begin{bmatrix} \mu_{ir_1j} & \mu_{ir_2j} & \dots \end{bmatrix}$, and

$\boldsymbol{\tau}_{imj}^\top = \begin{bmatrix} \tau_{ir_2j} & \tau_{ir_2j} & \dots \end{bmatrix}$, the vectors of market shares, markups, and iceberg trade costs along all routes carrying freight from i to j via m . Total profits are thus:

$$\Pi_{imj} = B_j \boldsymbol{\pi}_{imj}^\top [(\boldsymbol{\mu}_{imj} - \mathbf{1}) \circ \boldsymbol{\tau}_{imj}]$$

where B_j is the total spending of destination j , which the transporter treats as exogenous, and \circ denotes the element-wise matrix product. It follows that the transporter's marginal profit with respect to its vector of markups $\boldsymbol{\mu}_{imj}$ is given by:

$$\begin{aligned} \nabla \Pi_{imj} &= \frac{\partial \Pi_{imj}(\pi_{ir_1|j}, \pi_{ir_2|j}, \dots)}{\partial (\mu_{ir_1j}, \mu_{ir_2j}, \dots)} \\ &= \left(\frac{\partial (\ln \mu_{ir_1j}, \ln \mu_{ir_2j}, \dots)}{\partial (\mu_{ir_1j}, \mu_{ir_2j}, \dots)} \right) \left(\frac{\partial \Pi_{imj}(\pi_{ir_1|j}, \pi_{ir_2|j}, \dots)}{\partial (\ln \mu_{ir_1j}, \ln \mu_{ir_2j}, \dots)} \right) \\ &= B_j \left(\mathbf{DS}_{imj}^\top (\boldsymbol{\mu}_{imj} - \mathbf{1}) + \lambda_i \boldsymbol{\pi}_{imj} \right) \circ \frac{\boldsymbol{\tau}_{imj}}{\boldsymbol{\mu}_{imj}} \end{aligned}$$

where $\mathbf{DS}^\top = \begin{bmatrix} \frac{\partial \pi_{ir_1|j}}{\partial (\ln \mu_{ir_1j}, \ln \mu_{ir_2j}, \dots)} & \frac{\partial \pi_{ir_2|j}}{\partial (\ln \mu_{ir_1j}, \ln \mu_{ir_2j}, \dots)} & \dots \end{bmatrix}$ is the Jacobian matrix of trade shares with respect to the vector of log markups, while $\lambda_i \in [0, 1]$ captures the transporter's pricing conduct. This λ_i parameter reflects the ferocity of freight market competition for transport services out of i . $\lambda_i = 0$ corresponds to Bertrand competition: freight markets are perfectly competitive and markups as a percent of marginal cost go to 1. In contrast, λ_i parameters different from zero point to deviations from Bertrand competition, suggesting exercise of freight market power; at the extreme, $\lambda_i = 1$ corresponds to a perfect monopoly (oligopoly) in market i . This parameterization of the transporter's profit-maximizing behavior thus permits a wide variety of solution concepts.

Manipulating the transporter's first-order condition yields the pricing rule:

$$\begin{aligned} \mathbf{0} &= B_j \left(\mathbf{DS}_{imj}^\top (\boldsymbol{\mu}_{imj} - \mathbf{1}) + \lambda_i \boldsymbol{\pi}_{imj} \right) \circ \frac{\boldsymbol{\tau}_{imj}}{\boldsymbol{\mu}_{imj}} \\ \boldsymbol{\mu}_{imj} &= \mathbf{1} - \lambda_i (\mathbf{DS}_{imj}^\top)^{-1} \boldsymbol{\pi}_{imj} \\ \ln \boldsymbol{\mu}_{imj} &\approx -\lambda_i (\mathbf{DS}_{imj}^\top)^{-1} \boldsymbol{\pi}_{imj} \end{aligned}$$

where this last step follows from a first-order Taylor series expansion about 1. It will prove expedient

to define:

$$\boldsymbol{\delta}_{imj} = \begin{bmatrix} \delta_{ir_1j} \\ \delta_{ir_2j} \\ \vdots \end{bmatrix} = -\theta(\mathbf{DS}_{imj}^\top)^{-1} \boldsymbol{\pi}_{imj} \quad (16)$$

Thanks to the logit-demand structure, the \mathbf{DS}_{imj}^\top matrix may be easily calculated from the (observable) trade shares and correlation parameters; see Appendix A.3 for detail. Markups along an individual route are given by

$$\ln \mu_{irj} \approx (\lambda_i/\theta)\delta_{irj}. \quad (17)$$

I thus arrive at a simple, linear expression for markups that encompasses a wide array of solution concepts. Importantly, δ_{irj} may be easily calculated from observable data.

3 Empirical Strategy

Having laid out the theory, I turn my attention to estimating the model fundamentals. In this section, I demonstrate how the structure developed through Section 2 yields a simple, linear estimating equation that identifies: i) expected trade costs per mile, by mode; ii) the current severity of freight-market competition within and across distinct modes; and iii) the structural correlation parameters ρ and ζ . I also detail the data used to estimate the model. Notably, my model characterizes trade along individual routes, while the data are aggregated by origin, destination, port of entry/exit (if any), and mode; I thus develop and detail a method to estimate model fundamentals from aggregated data.

3.1 Data

I utilize domestic trade data from the Freight Analysis Framework, version 5 (FAF5), compiled by the Bureau of Transportation Statistics (BTS) and Federal Highway Administration (FHA). This dataset lists total annual trade volumes in 2017 disaggregated by mode among major metropolitan areas in the U.S. and the following international regions: Canada, Mexico, Rest of Americas, Europe, Africa, Southwest and Central Asia, Eastern Asia, Southeast Asia, and Oceania.¹⁸ The

¹⁸Unfortunately, the FAF does not offer more granular international geographies.

FAF also encompasses large, rural areas in each state. Figure 3 displays the domestic regions. I restrict my analysis of mode and route choice to the mainland U.S. due to the significant natural and political boundaries facing Hawaii and Alaska. For the same reasons, I do not model mode or route choice for the international portions of a journey. I thus analyse transportation among 129 domestic locations, as well as the eight international regions. The data are aggregated by origin, port of entry (for imports), port of exit (for exports), destination, and mode.¹⁹ I restrict my analysis to five domestic modes: Road, Rail, Water, Air, and Multi-Modal; I do not consider freight movements via pipeline or with an unknown domestic mode. I also remove trade flows valued at less than \$1 million total in 2017, to ensure enough variation in each origin-destination pairing to reliably identify the parameters of interest.

Second, I utilize detailed geographic information on the domestic transit network from the National Transportation Atlas Database (NTAD). The NTAD provides highly granular detail on domestic roadways, rail lines, navigable waterways, airports, and intermodal exchanges. I assume that travel may occur directly between any airport. Along the roadway, I limit my attention to arterial roads and interstates, as these carry the most interstate commerce. From these disparate modal networks, I create a graphical representation of a single, multi-modal transport network in PostgreSQL. Importantly, exchanges between modes may only occur at designated intermodal exchanges. Figure 2 provides a simplified example of my geography; Figure 4 displays a map of my network (excluding routes via international waters).

3.2 Estimating Model Parameters

I begin with my ideal regression specification. I parameterize the deterministic component of trade costs as follows:

$$\kappa_{r(m)} = Miles_r \beta_m, \quad (18)$$

where $Miles_r$ is the length of the route in thousands of miles, and β_m captures the expected cost per-mile along a particular mode. Plugging Equations (17) and (18) into Equation (12) yields the

¹⁹It is important to note that the air freight included in the FAF5 encompasses shipments that are serviced by both road and air. The reason for this aggregation is that air typically cannot perform final-mile services, and thus relies on trucks to complete the trip. This aggregation is not a problem when estimating my model, as I account for final-mile costs via destination \times mode fixed effects.

following log-linear expression:

$$\begin{aligned}\pi_{ir(e,x,m)|j} = \exp & \left(-\ln A_i - \lambda_i \delta_{irj} - \theta [\ln c_i + Miles_r \beta_m + u_{irj} + \eta_{ie} + \nu_{xj} + \alpha_{iem} + \gamma_{xmj}] \right. \\ & \left. + (1 - \varphi \rho \zeta) \ln \pi_{r|iexmj} + (1 - \rho \zeta) \ln \pi_{m|iexj} + (1 - \zeta) \ln \pi_{ex|ij} - Q_j \right). \quad (19)\end{aligned}$$

Given appropriate data, this expression provides a convenient, log-linear framework to estimate the model parameters.

3.2.1 Identification

Before detailing my estimation procedure, I must emphasize a few points regarding identification. First, because the log conditional probabilities $\ln \pi_{r|iexmj}$, $\ln \pi_{m|iexj}$, and $\ln \pi_{ex|ij}$ are included to identify the correlation coefficients, the cost and conduct parameters, β_m and λ_i , are identified by variation in trade shares across origins and destinations, which is observed, not simulated; similarly, ρ and ζ are respectively identified by observed variation in conditional trade shares across modes, domestic ports of entry. The parameter φ , however, cannot be identified, as it depends entirely on simulated variation; it does not reflect any observable variation in the data. Thus, I cannot empirically evaluate φ , but must fix it at the outset. Currently, I set this value to 1, implying zero correlation of transport efficiencies within origin, mode pairs. In Section 4.2, I show how the results change with lower values of φ (i.e. non-zero correlations among routes of the same origin, mode).

Second, Equation (19) makes evident that all cost coefficients are identified up to scale; I cannot separately identify θ . This scaling is not strictly a problem in the context of my model, but requires that I rely on estimates of θ from the literature when calibrating wages and performing counterfactual analysis. Henceforth, I assume a standard trade elasticity of 4.

Third, there is the obvious issue of endogeneity. The regressor δ_{irj} is endogenous for two reasons: i) the pricing rule laid out in Equations (16) and (17) makes clear that δ_{irj} is structurally correlated with u_{irj} , and ii) the linear approximation of markups introduces further error into the regression equation, which will necessarily be correlated with δ_{irj} . I overcome these identification problems with a classic instrumental variables strategy.

As an instrument, I propose the production cost of related goods, which, in this context, is the

distance of alternate routes. Explicitly, I utilize the following instrument:

$$Z_{irj} = \frac{1}{N} \sum_{\substack{e' \neq e \\ x' \neq x}} \sum_{r' \in \mathcal{R}_{e'x'}^m} \mathbb{1}(k(r') = k(r)) Miles_{r'} \quad (20)$$

where $\mathbb{1}()$ is the indicator function, $k(r)$ denotes the relative ordering of the route, and N is the dimensionality of the set. In words, I utilize the average mileage of competing trade routes carrying freight from i to j of the same relative ordering as r – so, the shortest path on Rail from e to x is instrumented by the average mileage of all shortest paths on Rail that carry trade from i to j that do not utilize e and x as their domestic ports of entry or exit. The second-shortest paths are instrumented analogously; and so on up to the longest path.

Of course, for my IV estimates to be valid, these instruments must satisfy the exclusion restriction and relevance assumptions. Regarding the former: the exclusion restriction is satisfied so long routed miles are independent of the error term, which holds by assumption in my theoretical setup. This strict independence is valid in reality if trade flows today are independent of the trade flows that influenced the planning and development of the disparate modal networks decades (or in some cases, centuries) ago. Moreover, many modal networks were built for reasons distinct from the efficient movement of goods: transportation of people, as well as national defense resources, are a major motivation underlying many transit networks, particularly the interstate highway system. Hence, my independence assumption seems reasonable. The relevance assumption holds so long as freight firms optimize prices across competing routes. This assumption follows directly from my theoretical setup and seems reasonable a priori – however, absent any price data from the transport industry, it is difficult to verify. The relevance of my proposed instruments may therefore be suspect – however, I may empirically evaluate the relevance of the instrument via the first-stage F-statistic (detailed in Panel D of Table 2). Reassuringly, all F-statistics suggest that my instruments are relevant.

3.2.2 Estimation

Given route-level data on domestic trade as well as knowledge of δ_{irj} , it would be straight-forward to estimate my model parameters via 2SLS. However, my data fails on both of these counts. As made evident by Equation (16) as well as Appendix A.3, δ_{irj} is a nonlinear function of φ and

ρ , which I aim to estimate in the same equation. Second, and much more problematic, I do not observe route-level trade shares; rather, my data only reports aggregate trade flows for an origin, destination, port of entry/exit (where relevant), and mode. I thus rely on a simulated method of moments strategy to overcome these data shortcomings.

As a first step, I populate the set \mathcal{R}_{ij}^m by mapping successively longer paths between e and x along each mode.²⁰ I also remove the first and last 25 miles from each journey, as these are the most-expensive parts of the trip and should be captured by the α_{iem} and γ_{jxm} parameters.²¹ Theoretically, I could repeat this process almost infinitely; practically, I consider only the 5 shortest paths for each mode. I have two, main reasons for stopping at this threshold: i) computation time grows with each additional route, becoming excessive after 5, and ii) routes outside of this set seem sufficiently circuitous to be cost-prohibitive, and therefore add little information to my analysis. This mapping process generates a set of 5 distinct routes – as well as the corresponding mileage – for domestic origin, destination, and mode combination.

Table 1 describes the evolution of average mileage across these subsequently longer routes for each mode. To construct this table, I scale the distance of each routing by the shortest distance for every domestic origin, destination, and mode pairing. I then average these scaled distances across origin-destination combinations to find the average, scaled distance for every routing. Columns (1) and (2) demonstrate that, on average, the second-shortest routing via Road is approximately 4.4% longer than the shortest path on the Road; the distance of the third-shortest path is 7.4% long than the shortest path, and 2.8% larger than the second-shortest path; and so on. Notably, for Roads, Rails, and Multi-modal, the marginal increase in mileage along each route generally shrinks as the number of routes increases; I attribute this trend to the relative density of these networks: as routes become more and more circuitous, the marginal increase in mileage becomes less and less. Likewise, the marginal increase in Air distance with each route is consistently small and stable; this trend owes to the fact that I allow a straight-line path between all freight airports, making the Air network the most dense by far. Finally, the increases in routed distance over Water are somewhat erratic, reflecting the relative sparsity of the water network. The last, notable takeaway

²⁰I require these paths to be substantially different, so that the changes to the distance are meaningful. Table 1 demonstrates the average evolution of mileage across these paths.

²¹This truncation, as well as the fact that I cannot route within a region, means that I hold $\kappa_r = 0$ for all routes that start and end in the same region.

from this table is the sizeable difference between the shortest path and the fifth-shortest path: for Roads and for Multi-modal, the tenth-shortest path is approximately 11-12% longer than the shortest path on average; this number hovers around 15% for the Rail and Water networks. For Air, the fifth-shortest path is only 1.3% greater than the shortest trip on average, again reflecting the unique ability of Air to travel in a straight line, anywhere.

The routed mileage identifies the per-mile cost parameters, β_m . The question now becomes how to estimate route-level costs (and markups), from aggregated data. Towards this end, I employ an Expectation-Maximization (EM) algorithm. The algorithm proceeds accordingly:

1. Take an initial guess at the model parameters, $\lambda_i^{(0)}, \beta_m^{(0)}, \zeta^{(0)}, \rho^{(0)}$, and $v^{(0)}$. Keep in mind that I have already fixed the parameters φ and θ .
2. (Expectation Step) Simulate $\mathbb{E} \left[\pi_{r|iexmj} \mid \lambda_i^{(0)}, \beta_m^{(0)}, \zeta^{(0)}, \rho^{(0)}, v^{(0)}, \varphi, \theta \right]$ according to Equation (4) under the assumption that $u_{irj} \sim N(0, v^{(0)})$. Denote this conditional probability $\pi_{r|iexmj}^{(0)}$.
3. Calculate $\pi_{ir|j}^{(0)} = \pi_{r|iexmj}^{(0)} \pi_{m|iexmj} \pi_{ex|ij} \pi_{i|j}$. Note that only the first of these conditional probabilities is simulated; the rest are observed in the data.
4. Calculate $\delta_{irj}^{(0)}$ as described by Equation (16) and Appendix A.3.
5. Estimate the first stage via OLS:

$$\delta_{irj}^{(0)} = Z_{irj} \zeta_m + Miles_r \phi_m + \vartheta_{iem} + \vartheta_{jxm} + \varepsilon_{irj}$$

where ϑ_{iem} and ϑ_{jxm} are fixed effects. Denote the fitted values from this regression $\hat{\delta}_{irj}^{(0)}$.

6. Define $y_{irj}^{(0)} = \ln \pi_{ir|j}^{(0)} - (1 - \varphi \rho^{(0)} \zeta^{(0)}) \ln \pi_{r|iexmj}^{(0)}$.
7. (Maximization Step) Estimate the second stage via OLS:

$$y_{irj}^{(0)} = -\theta Miles_r \beta_m - \lambda_i \hat{\delta}_{irj}^{(0)} + (1 - \rho \zeta) \ln \pi_{m|iexmj} + (1 - \zeta) \ln \pi_{ex|ij} - \theta u_{irj} + \underbrace{\text{Origin} \times \text{POE} \times \text{Mode FEs}}_{-\theta(\nu_{xj} + \gamma_{xjm}) - Q_j} + \underbrace{\text{Destination} \times \text{POX} \times \text{Mode FEs}}_{-\ln A_i - \theta(\ln c_i + \eta_{ie} + \alpha_{iem})} \quad (21)$$

Denote the new set of parameter estimates $\lambda_i^{(1)}, \beta_m^{(1)}, \zeta^{(1)}, \rho^{(1)}$, and $v^{(1)}$.²²

8. Return to step 2, and repeat the process with the new parameter estimates. Continue until the estimates converge.

Under standard assumptions required for a linear regression model, the parameter estimates of the EM process converge to the (local) maximum-likelihood estimates. See Appendix A.4 for further detail.

4 Descriptive Results

The end result of the EM process just laid out in Section 3.2 are estimated model fundamentals. Namely, these encompass per-mile iceberg cost coefficients β_m , the correlation parameters ρ and ζ , as well as the conduct parameters λ_i , which in turn inform route-level markups μ_{irj} . Table 2 summarizes the results of my favored specification; additional robustness checks and model validation exercises are discussed in Section 4.2.

4.1 Primary Specification

I begin discussion of my reduced-form estimates with Panel A of Table 2. This panel reports the parameter estimates that inform geographic costs in my trade model. I breakout per-mile costs by mode of transport, or – in the case of multi-modal – the cost a single transshipment. As these coefficients inform iceberg trade costs, direct interpretation is somewhat involved.²³ However, their magnitude and relative ordering align with similar estimates in the literature (Allen and Arkolakis, 2014; Donaldson, 2018; Allen and Arkolakis, 2022). Importantly, Road is estimated as the most expensive mode per-mile, followed by Rail and Water, which have similar magnitudes. Air is estimated as cheapest mode per-mile, which may prove initially surprising, given Air’s high fuel intensity and maintenance requirements. However, bear in mind that these estimated coefficients exclude first- and final-mile costs, as well as any costs accrued at a destination or origins.²⁴ The final reported coefficient in Panel A is a somewhat novel estimate: the cost of transshipment across modes. I estimate that the cost of a single transshipment accounts for approximately 1. 1% of the final value of a good. Note that this effect compounds across multiple exchanges.

I now shift focus to the estimated correlation coefficients listed in Panel B of Table 2. Note that these are inverse correlation coefficients: higher values of ρ, ζ imply lower correlations among

²²It should be noted that, while I do not immediately estimate $v^{(1)}$ via OLS, I can estimate $v^{(1)} = \text{Var}(\hat{u}_{irj})$.

²³Interpreting the first reported coefficient: 1,000 additional miles on road increases iceberg trade costs, τ_{irj} , by $\exp(0.197) \approx 1.218$, or about 21.8%. Interpretation of the remaining coefficients is analogous.

²⁴These route-invariant costs are estimated via fixed-effects in my regression specification. See Section 3 for detail.

composite efficiencies among modes, origins. Explicitly, the real correlation may be calculated as 1 minus the square of the estimated coefficient (Heiss, 2002). My estimate of ρ thus implies that, on average, transportation efficiencies – and hence, prices – across domestic modes enjoy a correlation of $1 - 0.596^2 = 0.645$; production efficiencies across domestic locations report a correlation of $1 - 0.379^2 = 0.856$. Both of these estimates are statistically distinct from 1, which implies zero correlation. These substantial correlation estimates underscore the importance of allowing correlation in my model. In Section 4.2, I explore the consequences of imposing zero correlation, as is common the conventional EK setting.

Panel C summarizes the distribution of estimated non-competitive markups $\hat{\mu}_{irj} = \hat{\lambda}_i \delta_{irj}$. I focus on the distribution of markups – as opposed to the distribution of conduct parameters λ_i – due to ease of interpretability.²⁵ The table demonstrates that, across all domestic trade routes, markups average 3.7% above marginal cost. The distribution is slightly skew right; the highest estimated markup is just over 13% above marginal cost.²⁶ These estimated markups are fairly low, suggesting that, in general, freight markets are highly competitive.

4.2 Robustness Checks

Forthcoming.

5 Counterfactual Simulations

Having estimated my bevy of fundamentals, I calibrate the model to domestic trade flows in 2017; I then run three counterfactual simulations, designed to highlight the role of freight transport in setting domestic trade outcomes. The first such exercise investigates which regions and modes are most/least impacted by imperfect competition in the market for freight transport. Explicitly, I compare calibrated welfare under a counterfactual, perfectly-competitive pricing regime to calibrated welfare under the status quo; this juxtaposition reveals where and along what modes current non-competitive losses are concentrated. My second counterfactual evaluates the welfare consequences

²⁵While the extreme cases of $\lambda_i = 1$ and $\lambda_i = 0$ are easily interpretable as perfect monopoly and perfect competition, intermediate values are more obscure. I thus focus discussion of my reduced-form results on the distribution of markups, as opposed to the conduct parameters themselves. A histogram of the estimated λ_i parameters is presented in figure ??.

²⁶I will analyze the geographic distribution of these markups – or rather, their consequences – in Section 5.

of removing an entire mode of transport from the domestic transit network: specifically, rail and (consequently) multi-modal.²⁷ This simulation is inspired by the proposed rail strike of 2022, which was narrowly avoided at the eleventh hour by federal intervention, much to the chagrin of labor unions (Shepardson and Baertlein, [November 29, 2022](#)). My model sheds light on the potential impacts of such a strike, how trade would have moved to competing modes, and how freight market power may amplify or attenuate downstream welfare losses to consumers. My final counterfactual simulates an international trade shock: specifically, a sharp increase in trade costs at international gates, meant to emulate supply chain bottlenecks sparked by the Covid-19 pandemic. This counterfactual reveals how strategic pricing across a geographically dispersed, multi-modal network exacerbates or mitigates an exogenous, geographically concentrated trade shock. Together, these three scenarios highlight how the transport sector influences domestic trade outcomes.

It is important to emphasize that my model is agnostic about the source of market power: I cannot differentiate between non-competitive pricing stemming from collusion or from barriers to entry. However, with the notable exception of Rail, freight markets are typically saturated with multiple service providers,²⁸ while fixed-costs in the industry are exceptionally high.²⁹ It thus appears likely a-priori that barriers to entry are the culprit for exercise of freight market-power; accordingly, I direct my policy discussion towards lowering barriers to entry, as opposed to anti-trust enforcement.

I now detail the results of my counterfactual simulations.

²⁷Why multi-modal as well? The lion's share of domestic multi-modal movement's encompass the rail network (AAR, [October, 2023](#)); hence, removing rail also vastly limits the scope for multi-modal travel. For the purpose of my counterfactual simulation, I make the simplifying assumption that, if Rail shuts down, multi-modal movements disappear as well.

²⁸In 2021, approximately 600 thousand for-hire interstate trucking companies operated in the United States (FMCSA, [2021](#)); approximately 543 air cargo carriers (FAA, [2021](#)), 37 U.S.-flagged maritime carriers (MARAD, [September, 2022](#)), and just 7 Class-1 freight railroads operated in the U.S. concurrently.

²⁹Trucking has the lowest entry cost: a new Semi truck runs between \$100 and \$200 thousand, with an additional \$50 thousand for a new trailer on average; this estimate excludes (substantial) insurance and licensing costs, as well as the cost of any sophisticated trailers – e.g., refrigeration, logging, HAZMAT, etc.. (Harris, [2021](#)). The remaining modes enjoy much higher fixed costs: a new diesel locomotive costs between \$1.5 to \$2 million on average (World Wide Rails, [2023](#)), while a new rail car runs between \$100 and \$150 thousand (Blaze, [2019](#)); a new cargo plane averages between \$49 and \$77 million, but can reach over \$400 million, depending on capacity and technology (Walsh, [2023](#)); and a newly-constructed container ship costs between \$14 and \$300 million, again depending on capacity and technology (UNCTAD, [2010](#)). In addition, while roads, waterways, and airways are (generally) free-to-use, rail companies must create and maintain their own infrastructure.

5.1 Simulating a Perfectly Competitive Freight Market

For this counterfactual exercise, I set log-markups to zero across all domestic trade routes; I then utilize Equations (4) - (17) to simulate trade flows and prices with this perfectly-competitive freight market. Comparing calibrated welfare under the status-quo and counterfactual pricing regimes reveals current losses due to non-competitive freight pricing. I further decompose these aggregate effects by mode and geography in Table 3 and Figure 6, respectively. The former exploits my logit structure to simulate substitution patterns across competing modes; the latter reveals what locations enjoy the greatest/least concentrations of freight market power, and thus stand the most/least to gain from an erosion of that pricing power. I now discuss these results in detail.

I find that, as a result of removing freight market power, real welfare in the U.S. increases by approximately 5.04%; Panel A of Table 3 details total welfare changes accruing to each mode and overall. Column (1) of the table lists the baseline share of real trade volumes; Column (4) details the percentage change in this trade share brought about by the imposition of perfect freight competition. Columns (2) and (3) decompose this aggregate change into a modal substitution and income effect. The former effect is calculated by simulating the change in trade volumes, holding constant income in each region;³⁰ the latter effect is calculated by simulating the change in aggregate trade volumes to each region, holding constant the distribution of trade across modes.³¹ The sum of these effects equals the total change in trade volume.

Analysis of Panel A, Column (2) reveals that, holding real incomes in each region constant, elimination of freight markups shifts trade away from multi-modal transport and onto the road. This result is initially surprising, as it suggests road transport currently enjoys the *highest* markups, despite having by-far the highest market concentration and barriers to entry. One potential explanation for this counter-intuitive outcome is the unique ability of truck transport to complete the first- and final-mile. This supreme routing flexibility limits the scope for cross-modal competition: no alternative save multi-modal can offer comparable services. Indeed, Column (2) displays that the vast majority of this new trucking volume comes from multi-modal; very little crosses over

³⁰If markups were uniformly distributed across modes, then the substitution effect would simply equal the change in trade costs multiplied by the baseline trade share of each mode.

³¹If markups were uniformly distributed across geography, then the income effect would simply equal the change in income multiplied by the baseline trade share.

from Rail, Water, or Air.³² Moreover, despite the vast number of trucking companies, anecdotal evidence suggests that driver shortages have left a large quantity of transport demand unmet.³³ In summary, Column (2) displays the imperfect substitution of trade across modes: price decreases that mainly affect the Road draw trade primarily from multi-modal.

I now shift attention to Panel A, Columns (3) and (4). The former isolates the income effect: the change in welfare brought about by making certain regions wealthier via a reduction in trade costs. This column aligns with expectation: all modes see an increase in real trade volumes, and the relative distribution of these increases roughly corresponds to the baseline trade allocation displayed in Column (1).³⁴ Finally, Column (4) presents the aggregate change in welfare accruing to each mode. Notably, the income effect dominates for all modes except multi-modal. Hence, the lion's share of welfare improvements accruing to each mode stems from these income gains following the reduction in trade costs.

Panels B and C of Table 3 repeat much the same exercise, focusing instead on imports and exports; the outcomes reported in these panels largely mirror the effects on domestic welfare. Focusing first on Column (2), roadways see the largest relative benefit holding income in each region constant. Among imports, these newfound roadway flows again draw primarily from multi-modal; among exports, this substitution effect pulls primarily from rail. In general, rail, air, and water see much higher substitution effects among international movements than among domestic trade, a trend likely attributable to their higher baseline trade volumes (see Column (1)). Column (3) demonstrates that, for both imports and exports, trucking is again the largest benefactor from the income effect; however, among exports, all modes report substantial increase in volume due to increasing incomes. Finally, in Column (4), I report aggregate changes: roadways again see the largest change in total imports and exports, driven largely by the income effect reported in Column (3). Total imports increase by 7.52%, while exports climb by nearly 20%. This outsize effect on

³²This explanation is admittedly speculative; absent more refined geographic data, I cannot evaluate this “final-mile hypothesis” empirically.

³³This labor shortage is stark enough that the American Trucking Associations released a “Driver Shortage Analysis” in 2019, and cited the lack of qualified drivers as the main culprit for supply chain disruptions in the trucking industry (Costello and Karickhoff, 2019); meanwhile, the Association of American Railways is promoting the ability of its intermodal network ease supply chain disruptions caused by truck-driver shortages (AAR, October, 2023). Moreover, the freight industry typically operates on tight timelines, which exacerbate the market power of available shippers.

³⁴Note that this relative distribution does not perfectly correspond to Column (1) due to geographic heterogeneity: as just discussed, the largest gains from this counterfactual are concentrated on the roadway; areas that trade more heavily in the road will see the largest income gains. Figure 6 provides a more detailed geographic analysis.

exports is striking, and suggests that managing freight market power is a powerful policy tool to influence our international trade balance.

Finally, in Figure 6, I breakout the geographic incidence of removing non-competitive freight rates. Panel A reports real welfare impacts: generally, the largest welfare gains accrue to rural areas in the Southeast and Mountain West, as well as to small urban areas in the Midwest and along the Gulf of Mexico. Strikingly, major international gates, including Los Angeles/Long Beach, CA, San Francisco/Oakland, CA, New York, NY, Chicago, IL, Baltimore, MD, Norfolk, VA, Atlanta, GA, and Ft. Lauderdale, FL, are among the *least* affected areas. While this result aligns with expectation – high trade volumes should attract more shippers, thereby reducing market power – it suggest that the aggregate impact of removing freight market power will be muted relative to the local impact in rural regions. Indeed, the Panel A of Figure 6 reveals that local impacts range from 2 to 11% of baseline welfare.

Panels B and C of Figure 6 report the geographic incidence among imports and exports, respectively. I begin with imports, where the largest gains accrue mostly to the coasts, as well as the northern Midwest and Great Plains. Regions up the middle of the country – including Lake Charles, LA, Austin, TX, Laredo, TX, East St. Louis, IL, Rural Georgia, Rural Indiana, most regions in Appalachia, and all of Michigan – experience modest increases or even *declines* in imports. Notably, these areas also saw substantial welfare gains due to elimination of markups; this pattern suggests that, thanks to the alleviation of freight market power, these regions import relatively less from abroad as domestic goods become cheaper. Switching focus to Panel C, increases in real exports accrue primarily to the regions bordering the Gulf of Mexico, as well as rural areas up the east coast and in the Northwest. There is not a discernable geographic relationship between welfare changes and export increases.

In summary, my first simulation explores the welfare consequences of removing freight market power. Most of these welfare gains accrue to the road, and shift domestic trade away primarily from multi-modal, and to a lesser extent, rail. This substitution pattern suggests that market power is currently concentrated along the roadway—an initially counter-intuitive finding that is somewhat supported by anecdotal evidence of a pervasive shortage of qualified truck drivers. Effects on international trade are similar, but larger. Most strikingly, real U.S. exports increase by nearly 20%, suggesting that freight market power has an outsize influence on the U.S. trade deficit. Geograph-

ically, gains from the simulation are concentrated in rural and small, urban areas throughout the Southeast, Midwest, and Gulf states; major international gates see the smallest welfare impacts. Notably, areas that see large welfare gains report the smallest gains or even modest declines in imports as a result of removing freight market power. This latter trend is likely the result of domestic freight becoming cheaper, leading to a lower reliance on imports.

5.2 Simulating a Rail Closure

While my first counterfactual is largely descriptive, the next is much more policy-focused. Explicitly, I simulate the effect of removing rail and multi-modal transport from the domestic transit network – this simulation emulates the narrowly-avoided rail strike of 2022. To highlight the role of freight-market concentration in determining domestic welfare, I simulate the shock twice: once under status quo freight pricing and once imposing perfect competition. Comparison of calibrated welfare under these two scenarios reveals how the downstream impacts of this exogenous shock are amplified/attenuated by market power in the freight industry.

Table 4 reports the impacts to domestic welfare as a result of removing rail and multi-modal. Panel A reports simulated welfare changes under status quo freight pricing; Panel B reports the same under perfect freight market competition. Comparison of these results reveals a key conclusion: removal of the railway (and consequently, multi-modal) leads to substantial welfare losses, regardless of freight market competition; however, losses are *worse* thanks to non-competitive freight pricing. Real welfare declines by 4.31% under the status quo, and only 2.86% under perfect competition. The reason for this substantial amplification stems from the exercise of market power: as displayed by Column (2), the vast majority of freight volumes shift onto the roadway, where freight market power is concentrated. Freight-service providers may then take advantage of the drop in cross-modal competition and raise prices. Column (3) reports welfare losses stemming from the effective change in income as a result of removing the railway. Note again that this income effect is concentrated in trucking. However, Panel (B) demonstrates that, absent an endogenous pricing response on behalf of freight carriers, welfare losses stemming from this income drop amount to only 2.77%. Hence, of the 4.23% drop reported in Panel A, approximately 1.46 percentage points – nearly 35% of the total change – is attributable to price increases stemming from a decline in modal competition. This income effect accounts for the majority of the aggregate changes reported

in Column (4).

Tables 5 and 6 repeat this exercise for real imports and exports. These results are very similar to the patterns exhibited for domestic welfare: losses are substantial, and made worse by the exercise of freight market power. Specifically, real imports decline by about 6.03% under perfect competition, and by 8% under status-quo pricing; real exports decline by approximately 1.23% under perfect freight market competition, and by 4.17% under the status-quo. The sharp difference in real export volumes is emblematic of the outsize effect freight market power exerts over exports, as previously discussed. The table demonstrates that the vast majority of international freight shifts to the road; however, in contrast to domestic welfare, a substantial share shifts to the air, especially among imports. Given the centrality of air and water transport to international transactions, this result is not surprising.

Finally, Figure 7 breaks out these real welfare changes by geography; Panel A reports results under status-quo freight pricing, and Panel B reports under perfect competition. Overall, losses are concentrated in the Southeast, northern Midwest, and Great Plains. Urban areas along the coast also report moderate losses. Notably, a handful of areas report welfare *gains* – these areas are served more readily by the road, air, and water networks, and thus see an increase in total trade volumes as trade shifts off the rail network. Comparison of Panels A and B reveals that exercise of freight market power exacerbates welfare losses among rural and small urban areas throughout the U.S.. This result is not surprising, as these areas report the highest concentrations of market power ex-ante. Geographic trends for imports and exports are similar, and reported in Figures ?? and ??.³⁵

In summary, shutting down the rail system would have a substantial, negative impact on domestic welfare; these losses are made worse by the exercise of market power along competing modes. I report similar impacts for imports and exports; most strikingly, freight market power has an outsize impact on exports—real export losses nearly quadruple under status-quo freight pricing relative to perfect freight market competition. Turning to the geographic incidence, losses are concentrated in the Southeast, northern Midwest, and Great Plains. Some areas, which are more heavily served the road, see *gains*. Exercise of freight market power exacerbates losses to rural and small urban

³⁵These results make clear that inland areas in the Great Plains are by-far the worst impacted among international trade flows.

areas throughout the country. Speaking broadly, these results emphasize that, should any, single mode shut down, we should expect a meaningful pricing response along competing modes, most especially trucking; this pricing response will most-impact rural and small urban areas.

5.3 Simulating an International Trade Shock

My final counterfactual explores how freight transport influences a geographically-concentrated international trade shock. Specifically, I simulate the welfare consequences of a 36% increase in trade costs along international routes, meant to emulate price increases witnessed during the Covid-19 pandemic.³⁶ This shock is geographically concentrated in the sense that only international gates feel the immediate impact; inland locations are not directly affected, but as I will demonstrate, suffer substantial losses due to equilibrium effects. I again simulate this shock twice: once under status quo freight pricing, and once under perfect freight market competition. Contrasting the changes in simulated welfare under these two pricing scenarios reveals the role of strategic freight pricing in determining domestic trade outcomes. More broadly, this counterfactual reveals how the freight industry influences the domestic welfare consequences of an international trade shock.

Table 7 reports real welfare changes from this simulation. Again, Panel A reports welfare impacts when the freight industry is allowed to exercise market power; Panel B reports welfare impacts under perfect freight market competition. In this case, we see that market power *attenuates* welfare changes, but very, very slightly. This result accords with expectation: market power implies imperfect pass-through of exogenous cost shocks; however, as demonstrated previously, freight market power is concentrated away from international gates. Hence, non-competitive freight pricing can have only a limited impact on international trade shocks. As displayed by Column (2), modal substitution effects are limited in magnitude, and concentrated along road and multi-modal, while air sees the largest (though still small) gains. Switching focus to Column (3), income effects are all negative and concentrated along the roadway. In total, domestic welfare declines by approximately 7.11% under status quo freight pricing, and 7.22% under perfect competition.

Unsurprisingly, this shock has a much larger impact on international trade. Tables 8 and 9 report simulated changes in real imports, exports under the status quo and perfect freight market

³⁶The magnitude of this shock comes from recent analysis by the St. Louis Federal Reserve (Leibovici, May 11, 2022).

competition. As reported in Panel B of each table, imports decline by approximately 17.97%, while exports decline by about 22.59% in the absence of freight market power. Attenuation rates due to non-competitive pricing are again minuscule, or even slightly negative: as reported in Panel A of each table, under the status-quo, imports decline by 17.84%, while exports decline by 22.67%. Focusing on Column (2), we see very little substitution across modes, implying a near-uniform shock across modes; this outcome is not surprising, as it is rare for an international gate to specialize in any, one mode. Column (3) reports substantial income effects; in-line with the uniform effect across modes, the relative distribution of these effects roughly corresponds to each mode's baseline trade share: Road sees the biggest declines, followed by multi-modal, air, rail, and finally, water.

The geographic distribution of the welfare impacts stemming from this shock are presented in Figure 10. Panel A reports real welfare changes under the status-quo, while Panel B reports welfare changes under perfect competition. Unsurprisingly, the two panels are nearly identical: rural Maine, Georgia, and Alabama, as well as East St. Louis, IL and Omaha, NE, report the only observable attenuation of welfare losses. Moreover, the figure reveals that Washington, Wyoming, Wisconsin, and West Virginia are the worst-impacted states in either pricing scenario: welfare losses in each of these states amount to at least 15%, and can climb as high as 20%. This geographic concentration is telling, as – with the exception of Washington – none of these states contain major international gates. Indeed, most international gates report small to moderate impacts. This finding suggests that rural, inland areas are worst impacted by an international trade shock. One explanation for this result is that major gates lie centrally in the domestic transit network, and are thus able to easily pick among cheaper suppliers/customers in response to more expensive foreign imports/exports. However, these increased costs are detrimental to rural areas along sparse portions of the network, who cannot easily adjust to consumption. Figures 11 and 12 breakout these effects for imports and exports and reveal largely the same pattern – the one, notable exception being for exports, where Florida reports the largest declines.

In summary, a sharp rise in international transport prices, similar to what the U.S. witnessed during the Covid-19 pandemic, creates substantial domestic welfare losses. These losses equal approximately 7% of baseline welfare, and are even more pronounced among imports and exports. Due to the concentration of freight market power away from international gates, this shock reports near-perfect pass through. Moreover, losses are generally concentrated within inland areas along

relatively sparse portions of the transit network; those locations along relatively dense portions of network more easily adjust production/consumption in response to the shock. These profound estimated losses buttress arguments in favor of forceful policy intervention in response to substantial international trade shocks: market forces will do little to attenuate the domestic welfare impacts, which could be extreme, and which will hit isolated, rural areas the hardest.

6 Conclusion

This paper quantifies the impact of the transport sector in setting domestic trade outcomes. I modify a standard Ricardian trade model to account for route-choice, mode-choice, port-choice, correlations across these disparate nests, and finally, imperfect competition for freight services in distinct markets. The net result of these refinements is a highly realistic model of the transportation industry, as well as its effect on domestic trade. The trade costs developed in my model reflect imperfect competition for freight services in distinct locations; imperfect substitution across origins, modes, and even parallel trade routes; and finally, available infrastructure. This framework allows me to evaluate the domestic welfare and trade incidence of a number of transportation shocks: i) removal of freight market power; ii) the complete removal of rail and (consequently) multi-modal transport; and iii) a sharp spike in international freight costs, similar to those witnessed during the Covid-19 pandemic. The model thus offers the most comprehensive view of how freight markets influence domestic trade outcomes.

I estimate fundamentals and calibrate the model to domestic trade flows in 2017. The former estimation yields the following insights: i) an estimate of per-mile trade costs along each mode; ii) the degree of correlation in prices across modes, origins; and iii) location-specific conduct parameters, which, in-turn, influence route-level markups throughout the domestic U.S.. The latter calibration yields 5 key insights: i) current losses due to non-competitive pricing are substantial, amounting to roughly 5% of baseline welfare; ii) the exercise of freight market power has an outsize impact on exports—elimination of freight market power could increase national exports by nearly 20%; iii) these impacts are concentrated in rural areas throughout the Southeast and Mountain West, as well as small urban areas in the Midwest and Gulf states; iv) exercise of freight market power exacerbates the impact of mode-specific shocks; and v) non-competitive freight pricing does

does little to attenuate international trade shocks, due to the concentration of freight market power away from international gates.

These results yield a number of insights relevant to policy-makers. First, losses due to non-competitive freight pricing are substantial, and somewhat surprisingly, concentrated in the trucking industry. Anecdotal evidence suggests that trucking in particular suffers from a shortage of qualified drivers, granting market power to existing operators. With the exception of multi-modal, competition from other modes is insufficient to solve this problem, as trucking offers the unique ability to fulfill the first- and final-mile. Hence, addressing the driver shortage is an obvious and immediate policy intervention, which will counter the vast majority of welfare losses due to non-competitive freight rates; further expansion of multi-modal terminals will also deflate the freight market power. Additionally, given the concentration of freight market power in rural and remote urban areas, such an intervention should help reduce economic inequality across the U.S.. Hence, actions to reduce barriers to entry in trucking will achieve the biggest impacts on domestic welfare.

Any policy intervention designed to deflate freight market power has import ramifications for the national trade deficit, which is of key interest to many politicians and policy makers. Because non-competitive freight pricing exerts an outsize influence on exports, it offers a heretofore unexplored lever to manage international trade flows. Importantly, it is a purely domestic policy, and does not require multilateral negotiation and enforcement.

Finally, the results of this model bulwark arguments in favor of aggressive policy interventions in response to transport shocks. Explicitly, the closure of the railway would lead to sizeable welfare losses, made worse by the exercise of market power from competing modes; an international trade shock is born almost exclusively by consumers – freight market power is concentrated away from international gates, and I estimate near-perfect pass through. Hence, sizeable intervention is necessary to avoid the worst welfare impacts of transport shocks.

Finally, it should be noted that, due to its centrality, transportation carries consequences far beyond trade flows. To name a few, the composition of freight carries environmental, health and safety, and equity concerns which are beyond the scope of this paper. A promising avenue for future research may apply the same method but analyse much different outcomes.

References

- AAR. (October, 2023). *AAR Intermodal Fact Sheet*. <https://www.aar.org/issue/freight-rail-intermodal/>
- Allen, T., & Arkolakis, C. (2014). Trade and the topography of the spatial economy. *The Quarterly Journal of Economics*, 129(3), 1085–1139.
- Allen, T., & Arkolakis, C. (2022). The welfare effects of transportation infrastructure improvements. *Review of Economic Studies*, 89(6), 2911–2957.
- Andri et mult. al., S. (2022). *DescTools: Tools for descriptive statistics* [R package version 0.99.47]. <https://cran.r-project.org/package=DescTools>
- Atkin, D., & Donaldson, D. (2015). *Who's getting globalized? the size and implications of intra-national trade costs* (Working Paper No. 21439). National Bureau of Economic Research. <https://doi.org/10.3386/w21439>
- Bache, S. M., & Wickham, H. (2022). *Magrittr: A forward-pipe operator for r* [R package version 2.0.3]. <https://CRAN.R-project.org/package=magrittr>
- Bergé, L. (2018). Efficient estimation of maximum likelihood models with multiple fixed-effects: The R package FENmlm. *CREA Discussion Papers*, (13).
- Berry, S. T. (1994). Estimating discrete-choice models of product differentiation. *The RAND Journal of Economics*, 25(2), 242–262.
- Blaze, J. (2019). *Railcar economics are as complex as the movement of freight*. Freight Waves. <https://www.freightwaves.com/news/economics-of-railcars-are-complex>
- Bonadio, B. (2021). *Ports vs. roads: Infrastructure, market access and regional outcomes* (tech. rep.). Working Paper.
- Brancaccio, G., Kalouptsidi, M., & Papageorgiou, T. (2020). Geography, transportation, and endogenous trade costs. *Econometrica*, 88(2), 657–691.
- Bresnahan, T. F. (1982). The oligopoly solution concept is identified. *Economics Letters*, 10(1–2), 87–92.
- Bureau of Transportation Statistics and Federal Highway Administration, U.S. DOT. (2022). *Freight analysis framework version 5 (faf5) regional database* [Accessed September 06, 2022]. https://faf.ornl.gov/faf5/data/download_files/FAF5.3.zip

- Coşar, A. K., & Demir, B. (2018). Shipping inside the box: Containerization and trade. *Journal of International Economics*, 114(100), 331–345. <https://doi.org/10.1016/j.jinteco.2018.07>
- Costello, B., & Karickhoff, A. (2019). *Truck driver shortage analysis* (tech. rep.). American Trucking Associations.
- Donaldson, D. (2018). Railroads of the raj: Estimating the impact of transportation infrastructure. *American Economic Review*, 108(4–5), 899–934.
- Donaldson, D., & Hornbeck, R. (2016). Railroads and american economic growth: A “market access” approach. *The Quarterly Journal of Economics*, 131(2), 699–858.
- Dowle, M., & Srinivasan, A. (2023). *Data.table: Extension of ‘data.frame’* [R package version 1.14.8]. <https://CRAN.R-project.org/package=data.table>
- Ducruet, C., Juhász, R., Nagy, D. K., & Steinwender, C. (2020). *All aboard: The effects of port development* (Working Paper No. 28148). National Bureau of Economic Research. <https://doi.org/10.3386/w28148>
- Eaton, J., & Kortum, S. (2002). Technology, geography, and trade. *Econometrica*, 70(5), 1741–1779.
- FAA. (2021). *All air cargo carriers in the u.s.* (tech. rep.). Federal Aviation Administration. https://www.faa.gov/sites/faa.gov/files/airports/planning_capacity/passenger-allcargo-stats/reporting/all-cargo-carriers-cy-2021.pdf
- Faber, B. (2014). Trade integration, market size, and industrialization: Evidence from china’s national trunk highway system. *Review of Economic Studies*, 81(3), 1046–1070.
- FMCSA. (2021). *Pocket guide to large truck and bus statistics* (tech. rep.). Federal Motor Carrier Safety Administration, U.S. Department of Transportation.
- Fuchs, S., & Wong, W. F. (2023). *Multimodal transport networks* (Federal Reserve Bank of Atlanta Working Paper # 2022-13).
- Ganapati, S., Wong, W. F., & Ziv, O. (2021). *Entrepot: Hubs, scale, and trade costs* (tech. rep.). National Bureau of Economic Research.
- Harris, S. (2021). *How much does a semi truck cost?* Freight Waves Ratings. <https://ratings.freightwaves.com/how-much-does-a-semi-truck-cost/>
- Heiss, F. (2002). Structural choice analysis with nested logit models. *Stata Journal*, 2(3), 227–252. <https://EconPapers.repec.org/RePEc:tsj:stataj:v:2:y:2002:i:3:p:227-252>

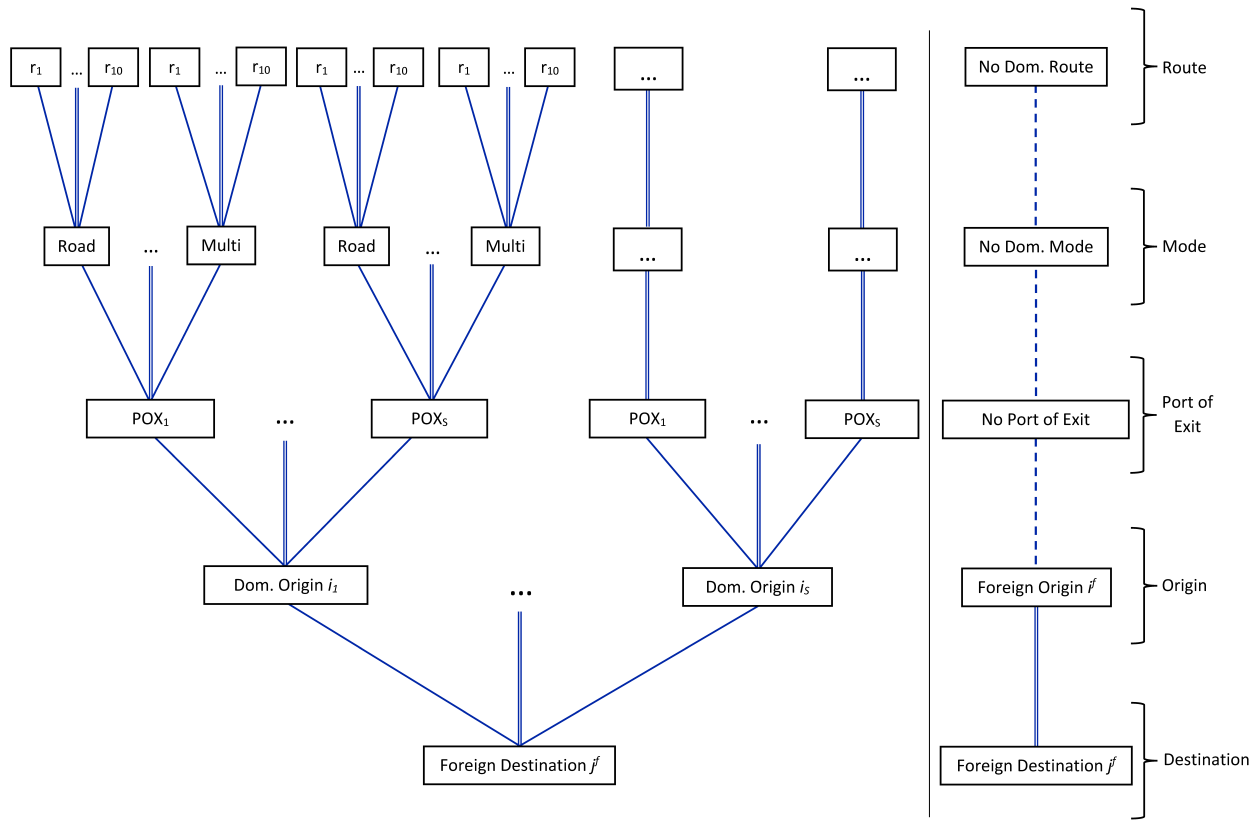
- Jaworski, T., Kitchens, C., & Nigai, S. (2022). *Highways and globalization* (NBER Working Paper # 27938).
- Kahle, D., & Wickham, H. (2013). Ggmap: Spatial visualization with ggplot2. *The R Journal*, 5(1), 144–161. <https://journal.r-project.org/archive/2013-1/kahle-wickham.pdf>
- Leibovici, F. (May 11, 2022). International shipping costs during and after covid-19. *Timely Topics (St. Louis Federal Reserve podcast)*. <https://www.stlouisfed.org/timely-topics/is-covid-19-sole-cause-of-shipping-disruptions-delays>
- Lind, N., & Ramondo, N. (2023). Trade with correlation. *American Economic Review*, 113(2), 317–53. <https://doi.org/10.1257/aer.20190781>
- MARAD. (September, 2022). *Contact information for u.s.-flag carriers* (tech. rep.). Maritime Administration, Office of Cargo Commercial Sealift. %7B<https://www.maritime.dot.gov/sites/marad.dot.gov/files/2022-09/U.S.-flag%20Contact%20List%20Sept%202022.pdf%7D>
- McFadden, D. L. (1984). Econometric analysis of qualitative response models. In Z. Griliches & M. Intriligator (Eds.), *Handbook of econometrics*. Elsevier Science Publishers.
- Microsoft, & Weston, S. (2022a). *Doparallel: Foreach parallel adaptor for the 'parallel' package* [R package version 1.0.17]. <https://CRAN.R-project.org/package=doParallel>
- Microsoft, & Weston, S. (2022b). *Foreach: Provides foreach looping construct* [R package version 1.5.2]. <https://CRAN.R-project.org/package=foreach>
- Miller, N. H., & Weinberg, M. C. (2017). Understanding the price effects of the millercoors joint venture. *Econometrica*, 85(6), 1763–1791. Retrieved April 28, 2023, from <http://www.jstor.org/stable/44955182>
- R Core Team. (2022). *R: A language and environment for statistical computing*. R Foundation for Statistical Computing. Vienna, Austria. <https://www.R-project.org/>
- Samuelson, P. A. (1954). The transfer problem and transport costs, ii: Analysis of effects of trade impediments. *The Economic Journal*, 64(254), 264–289. Retrieved May 30, 2023, from <http://www.jstor.org/stable/2226834>
- Shepardson, D., & Baertlein, L. (November 29, 2022). U.S. House to Vote to Block Rail Strike Despite Labor Objections. *Reuters*.
- Stubner, R. (2021). *Dqrng: Fast pseudo random number generators* [R package version 0.3.0]. <https://CRAN.R-project.org/package=dqrng>

- Train, K. E., McFadden, D. L., & Ben-Akiva, M. (1987). The demand for local telephone service: A fully discrete choice model of residential calling patterns and service choices. *The RAND Journal of Economics*, 18(1), 109–123.
- UNCTAD. (2010). *Review of maritime transport (2010)* (tech. rep.). United Nations Conference on Trade and Development.
- Walsh, S. (2023). *How much does a cargo plane cost?* Pilot Passion. <https://pilotpassion.com/how-much-does-a-cargo-plane-cost/>
- Wickham, H. (2022). *Stringr: Simple, consistent wrappers for common string operations* [R package version 1.5.0]. <https://CRAN.R-project.org/package=stringr>
- Wickham, H., François, R., Henry, L., & Müller, K. (2022). *Dplyr: A grammar of data manipulation* [R package version 1.0.10]. <https://CRAN.R-project.org/package=dplyr>
- Wickham, H., Ooms, J., & Müller, K. (2023). *Rpostgres: Rcpp interface to postgresql* [R package version 1.4.5]. <https://CRAN.R-project.org/package=RPostgres>
- World Wide Rails. (2023). *How much do locomotives cost?* <https://worldwiderails.com/how-much-do-locomotives-cost/>
- Wu, C. J. (1983). On the convergence properties of the em algorithm. *The Annals of Statistics*, 11(1), 95–103.

7 Figures & Tables

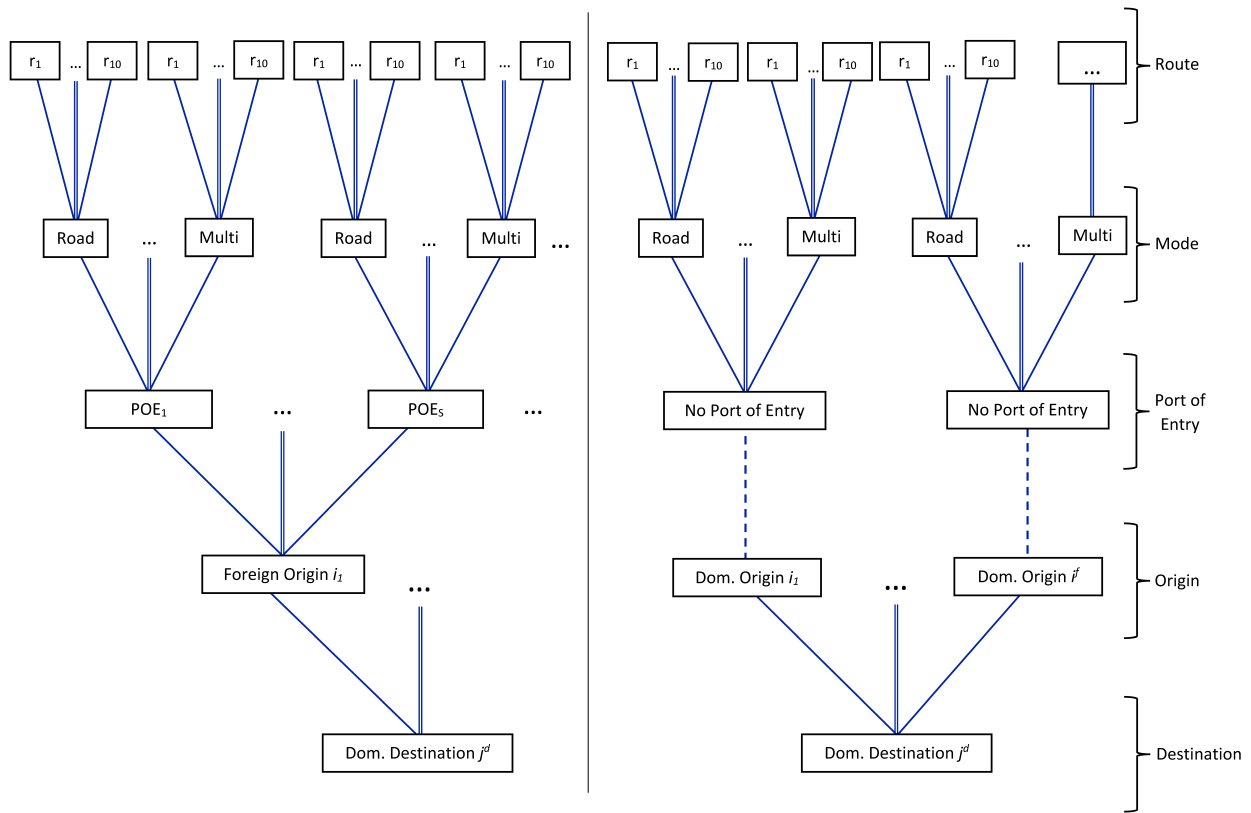
Figure 1: Details of the Nesting Structure

(a) Foreign Destinations



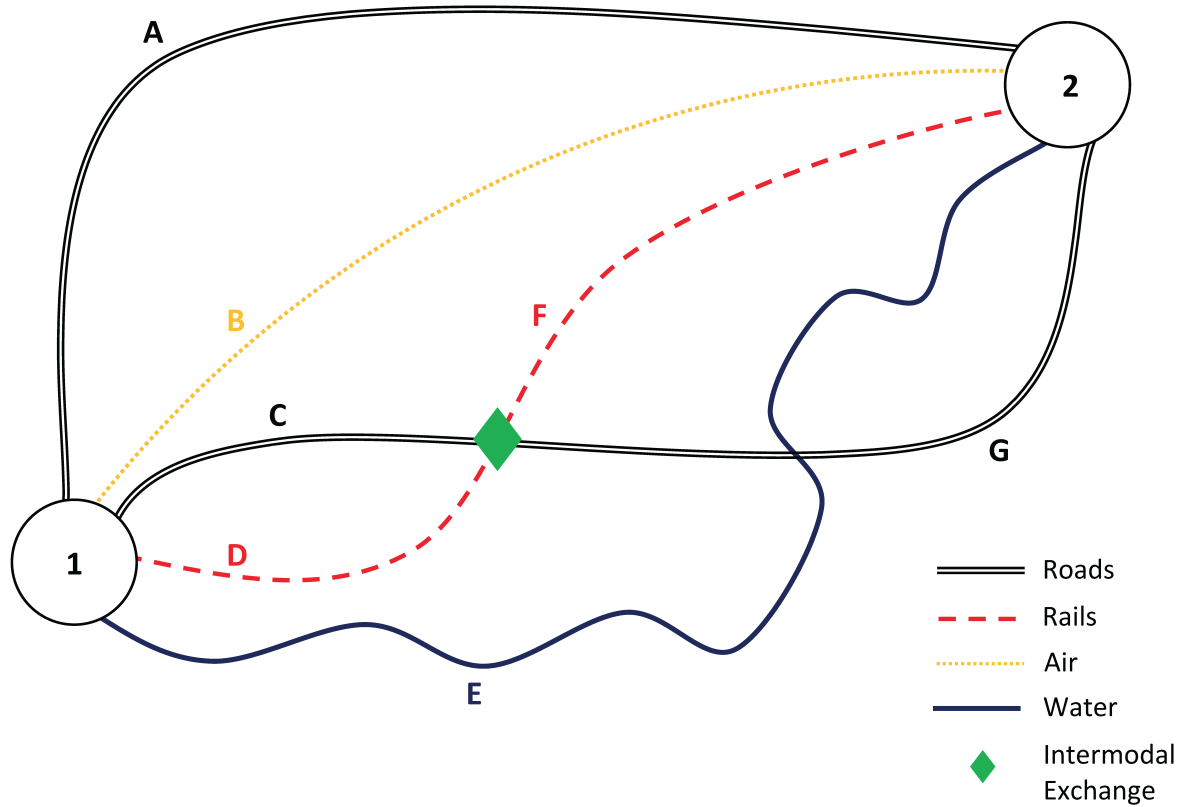
Continued on next page...

(b) Domestic Destinations



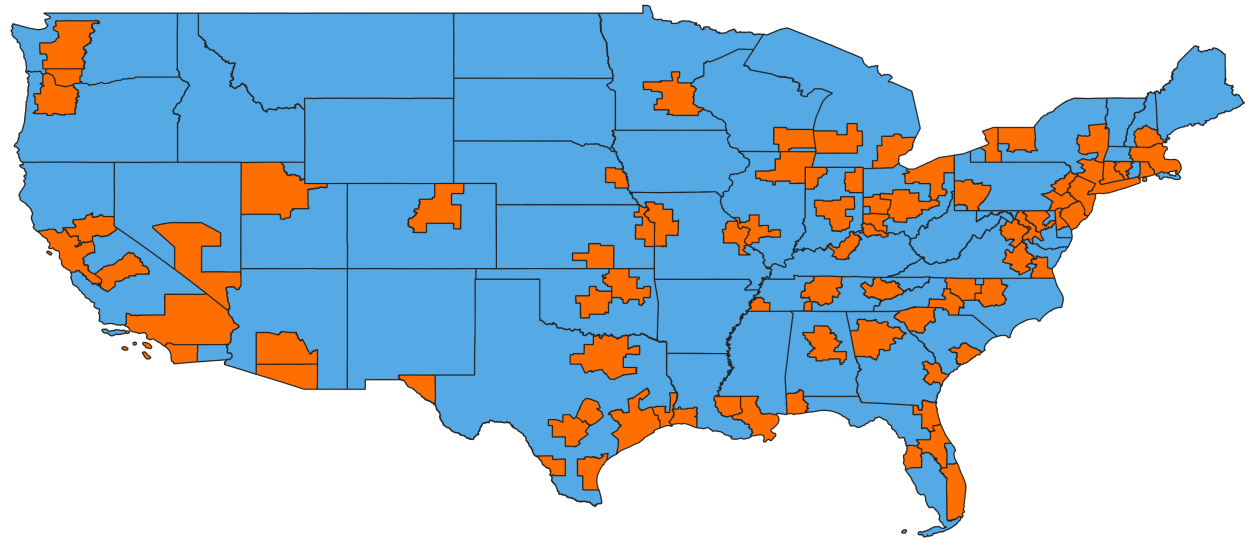
Notes: Panel A presents the nesting structure for foreign destinations; panel B presents the nesting structure for domestic destinations. Multiple options are presented as a compound line; degenerate branches are represented by a dashed line. Note that if a foreign destination elects a foreign origin, the tree becomes completely degenerate thereafter. Similarly, if a domestic location elects a domestic origin, the choice of port of entry/exit becomes degenerate (as there is no choice).

Figure 2: A Simple Network



Notes: The above figure displays a simplified transport network to illustrate the basic logic of my setup. In this case, $\mathcal{S}^d = \{1, 2\}$, and the sets of simple (non-repeating) routes along each mode are given by: $\mathcal{R}_{ex}^{Road} = \{A, CG\}$, $\mathcal{R}_{ex}^{Rail} = \{DF\}$, $\mathcal{R}_{ex}^{Air} = \{B\}$, $\mathcal{R}_{ex}^{Water} = \{E\}$, and $\mathcal{R}_{ex}^{Multi-modal} = \{A, CF, CG, DF, DG\}$. An important point regarding multi-modal: intermodal transshipment may only occur at designated intermodal exchanges (e.g. the green diamond); hence, even though the road network crosses a waterway, an exchange is not possible at this point. Additionally, multi-modal routes need not utilize the intermodal exchange. The defining feature of multi-modal is the *ability* to move across multiple networks, but not a requirement.

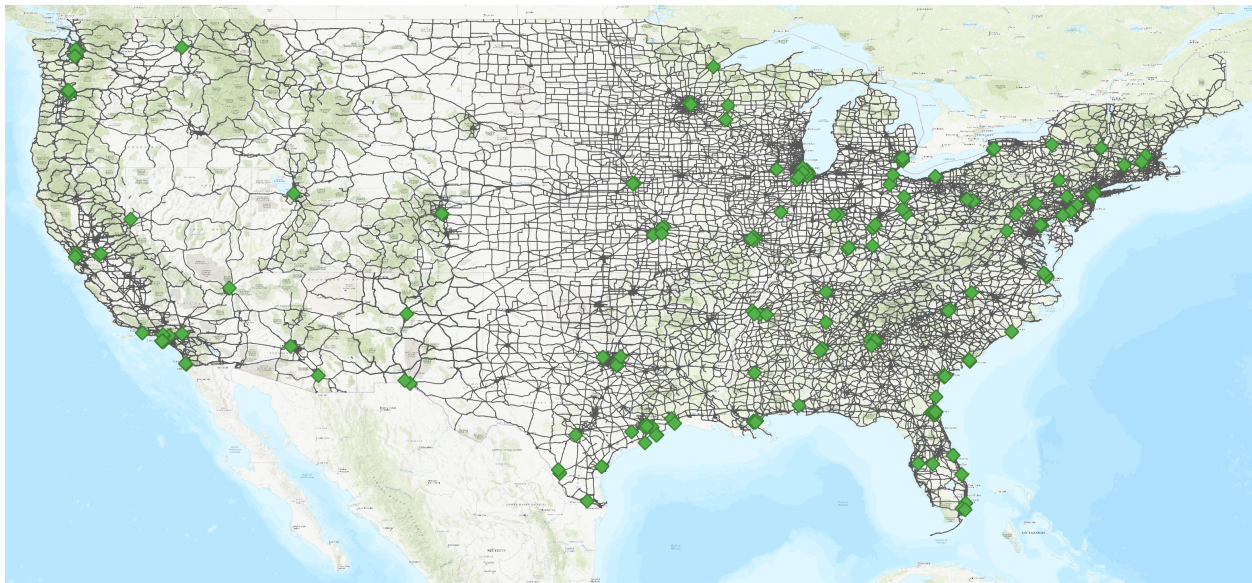
Figure 3: FAF Regions



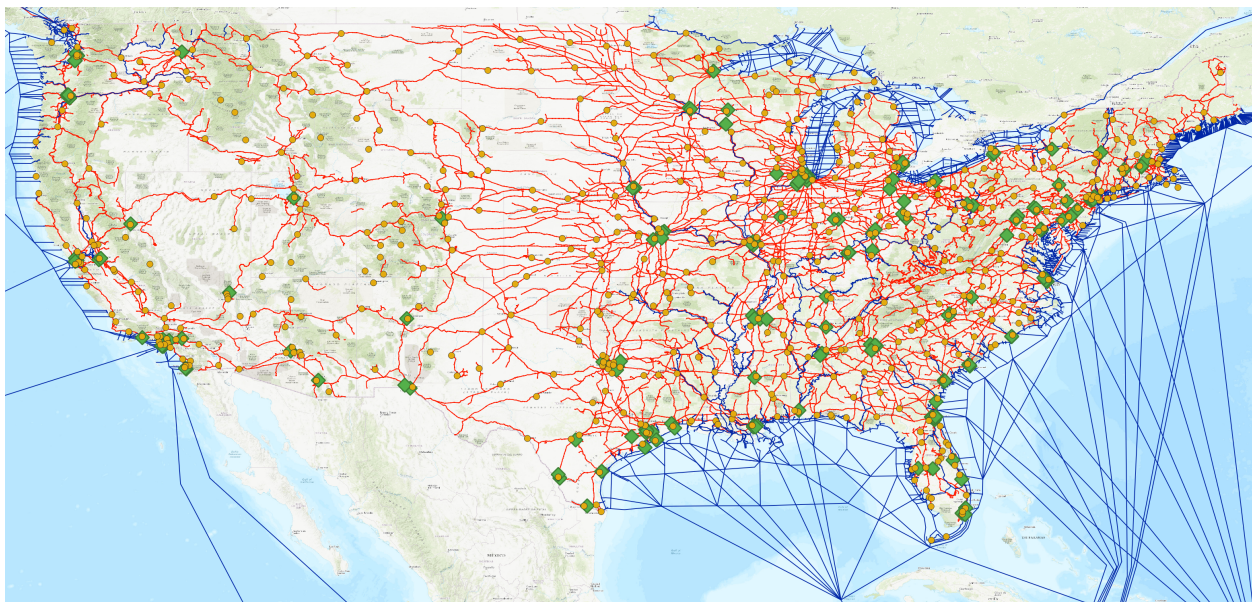
Notes: Black lines denote boundaries between regions. Bright orange areas denote major metropolitan areas. Light blue areas encompass large, rural areas. Note that there is at least one large, rural swath per state; rural areas are distinguished by their state.

Figure 4: National Transport Network

(a) Roads & Intermodal



(b) Rail, Water, Air, & Intermodal



Notes: This figure displays the domestic transport network in the mainland U.S.. Roads are depicted in dark grey, rails in red, navigable waterways in dark blue, airports accepting freight as golden-yellow points, and intermodal exchanges as green diamonds. Panels are split to make the separate networks clearer. Multi-modal transshipment may only occur at designated intermodal exchanges. I assume that travel may occur in a straight line between airports. Background map provided by ESRI World Topographical map.

Table 1: Evolution of Routed Mileage by Mode

Route	Road		Rail		Water		Air		Multi-modal	
	(1)	(2)	(3)	(4)	(5)	(6)	(7)	(8)	(9)	(10)
1	1	-	1	-	1	-	1	-	1	-
2	1.044	+4.4%	1.055	+5.5%	1.042	+4.2%	1.002	+0.2%	1.043	+4.3%
3	1.074	+2.8%	1.095	+3.8%	1.066	+2.3%	1.005	+0.3%	1.069	+2.5%
4	1.099	+2.3%	1.122	+2.4%	1.135	+6.5%	1.009	+0.4%	1.093	+2.2%
5	1.119	+1.8%	1.154	+2.9%	1.153	+1.6%	1.013	+0.4%	1.114	+1.9%

Notes: This table displays the average evolution of mileage along each route across all origin-destination pairs by mode. The odd-numbered columns display the average, scaled mileage per route; the shortest path takes a value of 1 for all origin-destination pairs. The even-numbered columns display the incremental percentage change in this average, scaled mileage.

Table 2: Estimated Fundamentals

A. Geographic Costs $\hat{\beta}_m$				
per-Mile Costs				Multi-Modal Exchange
Road	Rail	Water	Air	
0.197*** (0.018)	0.118*** (0.020)	0.124** (0.046)	0.087*** (0.013)	0.011*** (0.003)

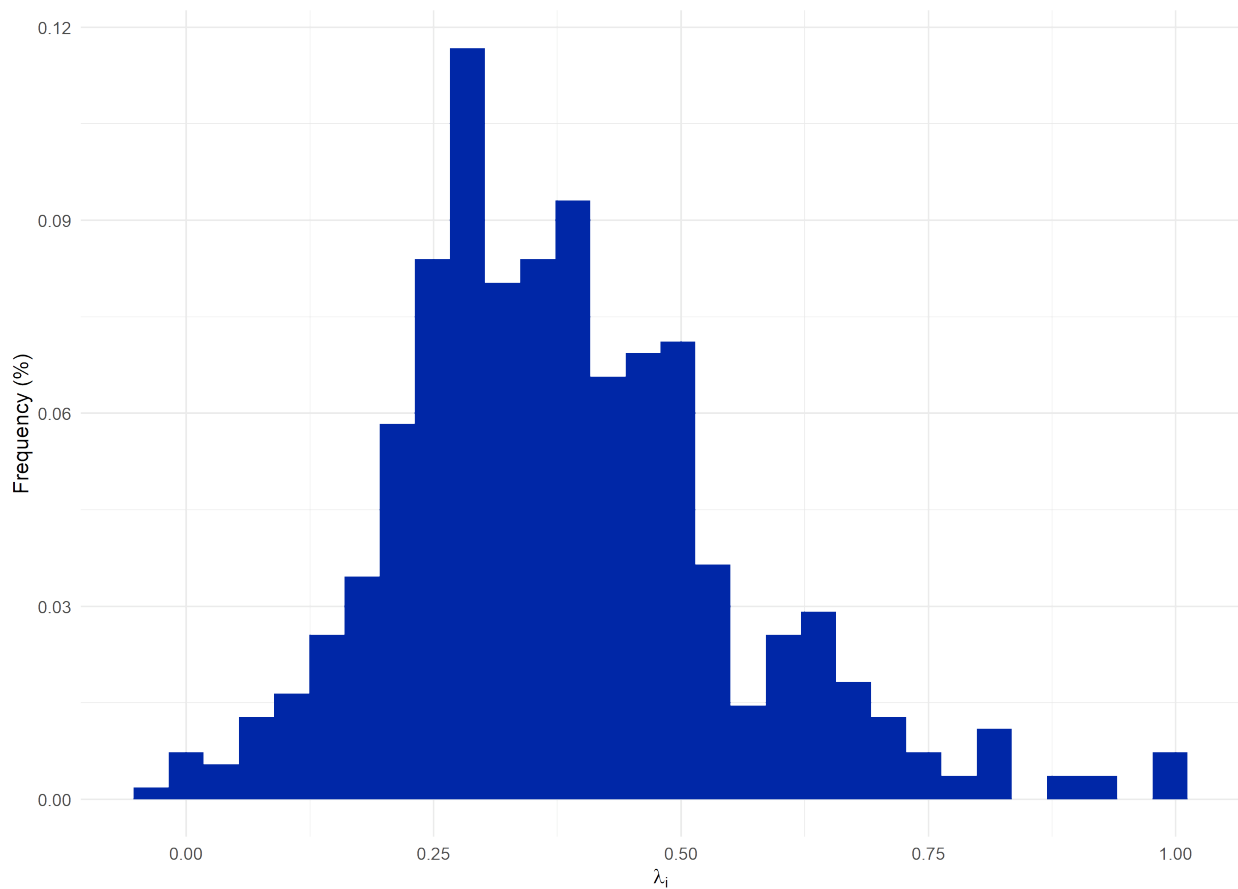
Route Correlation φ	Mode Correlation $\hat{\rho}$	Port Correlation $\hat{\zeta}$
1	0.596*** (0.013)	0.379*** (0.009)

Min	P25	P50	P75	Max	Mean	Std. Dev.
1.0000 (0.014)	1.023* (0.014)	1.032** (0.018)	1.045*** (0.020)	1.134*** (0.033)	1.037*** (0.019)	0.022*** (0.004)

N	Adj. R^2	First-Stage F -stat
397,435	0.919	31.887

Regression specification utilizes 5 routings per mode and are run with Origin \times POE \times Mode and Destination \times POX \times Mode FEs. Bootstrapped standard errors utilizing 500 iterations presented in parentheses. ***, **, and * respectively denote 0.1%, 1%, and 5% significance. Note that, in Panels B and C, I report significance tests relative to the null of 1. All parameter estimates assume a trade elasticity of 4.

Figure 5: Histogram of Estimated Conduct Parameters



Notes: This figure displays the distribution of my estimated conduct parameters. All estimates assume a trade elasticity of 4, and utilize my favored specification, which encompasses 5 potential routings per origin-destination-mode combination. Note that all estimates are normalized to span the [0, 1] range.

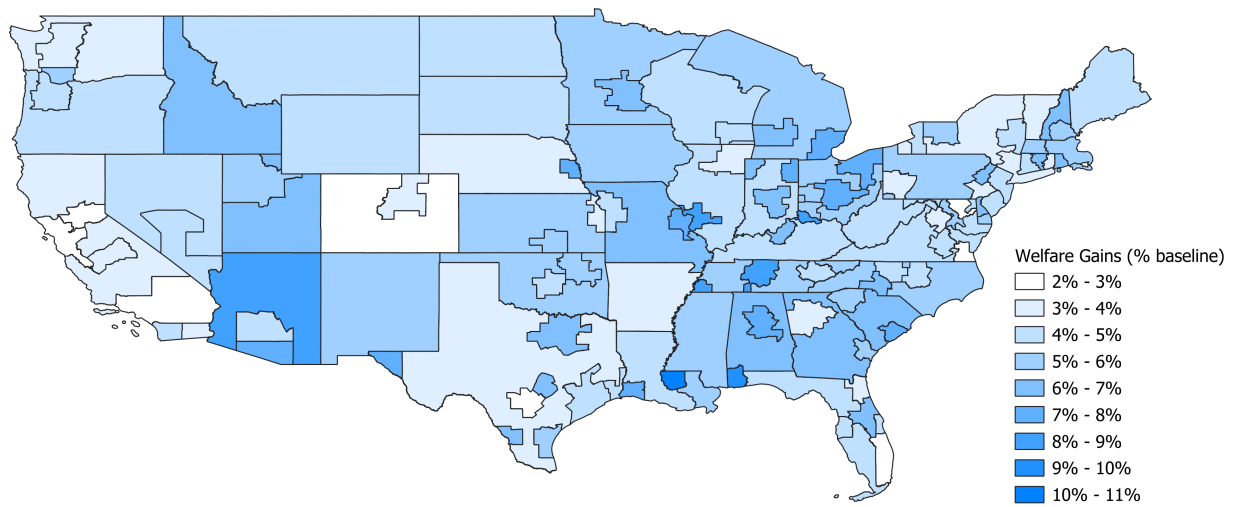
Table 3: Change in Real Welfare, Imports, and Exports under Perfect Freight Competition

	Baseline Trade Share (%)	Subs. Effect (ppt)	Income Effect (ppt)	Total Change (ppt)
	(1)	(2)	(3)	(4)
A. National Welfare				
Road	78.84	1.85	4.14	5.99
Rail	3.79	-0.17	0.12	-0.04
Water	1.61	0.16	0.13	0.28
Air	1.95	-0.18	0.14	-0.05
Multi	13.82	-1.65	0.52	-1.13
Total	100.00	0.00	5.04	5.04
B. Real Imports				
Road	60.72	3.37	5.22	8.59
Rail	9.53	-0.88	0.15	-0.72
Water	3.35	-0.25	0.16	-0.09
Air	10.27	-0.78	0.81	0.03
Multi	16.13	-1.46	1.18	-0.28
Total	100.00	0.00	7.52	7.52
C. Real Exports				
Road	67.03	1.96	13.59	15.54
Rail	11.39	-1.51	1.58	0.07
Water	8.20	0.11	2.39	2.50
Air	6.33	-0.14	0.99	0.85
Multi	7.05	-0.42	1.29	0.87
Total	100.00	0.00	19.84	19.84

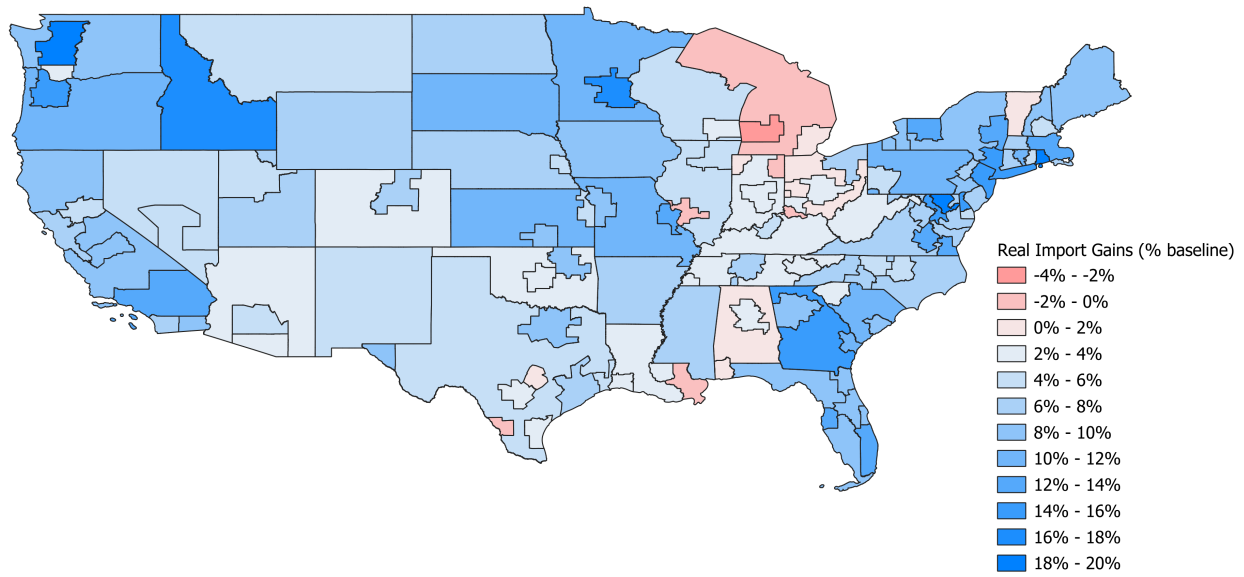
Notes: This table displays changes in real welfare accruing to each mode stemming from elimination of non-competitive pricing in the transport sector. Column (1) displays each mode's share of national trade in baseline, and is included for reference; Column (2) lists the change in trade volumes across modes, holding incomes constant; Column (3) lists the change in trade volumes resulting from a change in income, holding mode, route, and port choices constant; Column (4) = Column (2) + Column (3) lists the total change in transport volume (as a percent of national welfare) along each mode. The simulated changes are calculated using 5 potential routings for each mode-origin-destination combination.

Figure 6: Geographic Incidence from Elimination of Non-Competitive Markups

(a) Welfare

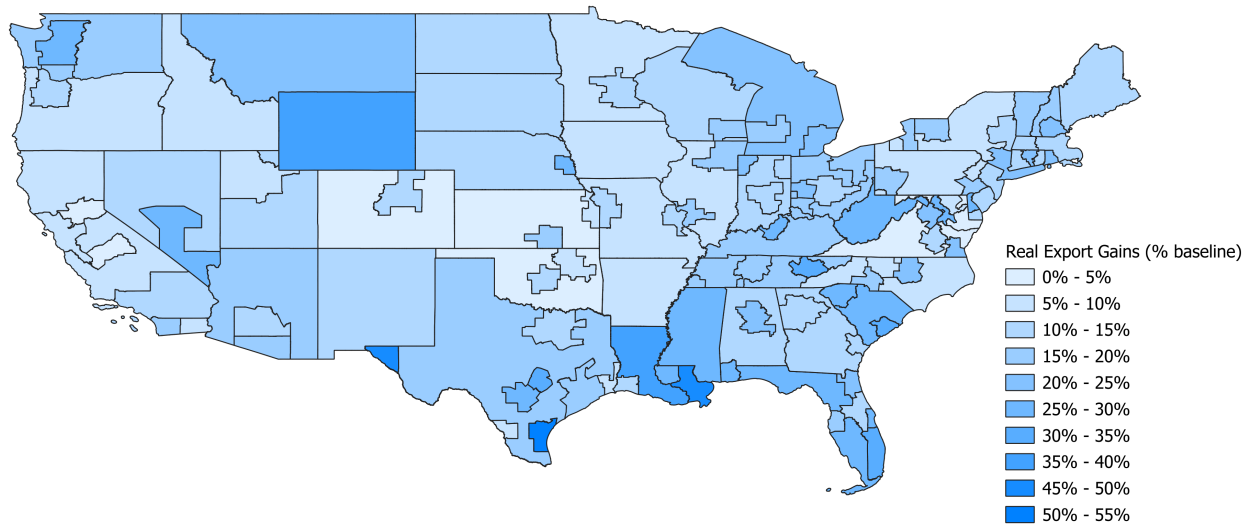


(b) Imports



Continued on next page...

(c) Exports



Notes: This figure presents potential change in real welfare, imports, and exports from imposing perfect competition in the transportation sector. These changes are calculated as the percentage increase in real welfare/ imports/ exports when eliminating markups over real welfare/ imports/ exports under the status quo. Darker colors signify greater changes—red denotes a decline in value, while blue denotes a gain.

Table 4: Change in Real Welfare under a Rail Strike

	Baseline Trade Share (%)	Subs. Effect (ppt)	Income Effect (ppt)	Total Change (ppt)
	(1)	(2)	(3)	(4)
A. Status-Quo Freight Pricing				
Road	78.84	15.91	-3.90	12.01
Rail	3.79	-3.79	0.00	-3.79
Water	1.61	0.34	-0.02	0.32
Air	1.95	1.27	-0.30	0.97
Multi	13.82	-13.82	0.00	-13.82
Total	100.00	-0.08	-4.23	-4.31
B. Perfect Freight Market Competition				
Road	80.75	14.43	-2.50	11.93
Rail	3.57	-3.57	0.00	-3.57
Water	1.80	0.32	-0.04	0.28
Air	1.81	0.79	-0.22	0.57
Multi	12.07	-12.07	0.00	-12.07
Total	100.00	-0.09	-2.77	-2.86

Notes: This table displays national welfare changes stemming from removal of rail and multi-modal transport. Column (1) displays each mode's share of national trade in baseline, and is included for reference; Column (2) lists the change in trade volumes across modes, holding incomes constant— note that, in this case, due to imperfect modal substitution and the elimination of certain modes, Column (2) need not sum to 0; Column (3) lists the change in trade volumes resulting from a change in income, holding mode, route, and port choices constant; Column (4) = Column (2) + Column (3) lists the total change in transport volume (as a percent of national welfare) along each mode. The simulated changes are calculated using 5 potential routings for each mode-origin-destination combination.

Table 5: Change in Real Imports under a Rail Strike

	Baseline Trade Share (%)	Subs. Effect (ppt)	Income Effect (ppt)	Total Change (ppt)
	(1)	(2)	(3)	(4)
A. Status-Quo Freight Pricing				
Road	60.72	18.58	-6.13	12.46
Rail	9.53	-9.53	0.00	-9.53
Water	3.35	1.51	-0.43	1.08
Air	10.27	5.57	-1.44	4.13
Multi	16.13	-16.13	0.00	-16.13
Total	100.00	-0.01	-7.99	-8.00
B. Perfect Freight Market Competition				
Road	64.46	17.52	-4.25	13.28
Rail	8.19	-8.19	0.00	-8.19
Water	3.02	1.30	-0.52	0.78
Air	9.57	4.11	-1.25	2.86
Multi	14.75	-14.75	0.00	-14.75
Total	100.00	-0.01	-6.02	-6.03

Notes: This table displays aggregate real import changes stemming from removal of rail and multi-modal transport. Column (1) displays each mode's share of national trade in baseline, and is included for reference; Column (2) lists the change in trade volumes across modes, holding incomes constant— note that, in this case, due to imperfect modal substitution and the elimination of certain modes, Column (2) need not sum to 0; Column (3) lists the change in trade volumes resulting from a change in income, holding mode, route, and port choices constant; Column (4) = Column (2) + Column (3) lists the total change in transport volume (as a percent of national welfare) along each mode .Panel A lists the change under status-quo freight pricing, while Panel B lists the change under perfect freight market competition. The simulated changes are calculated using 5 potential routings for each mode-origin-destination combination.

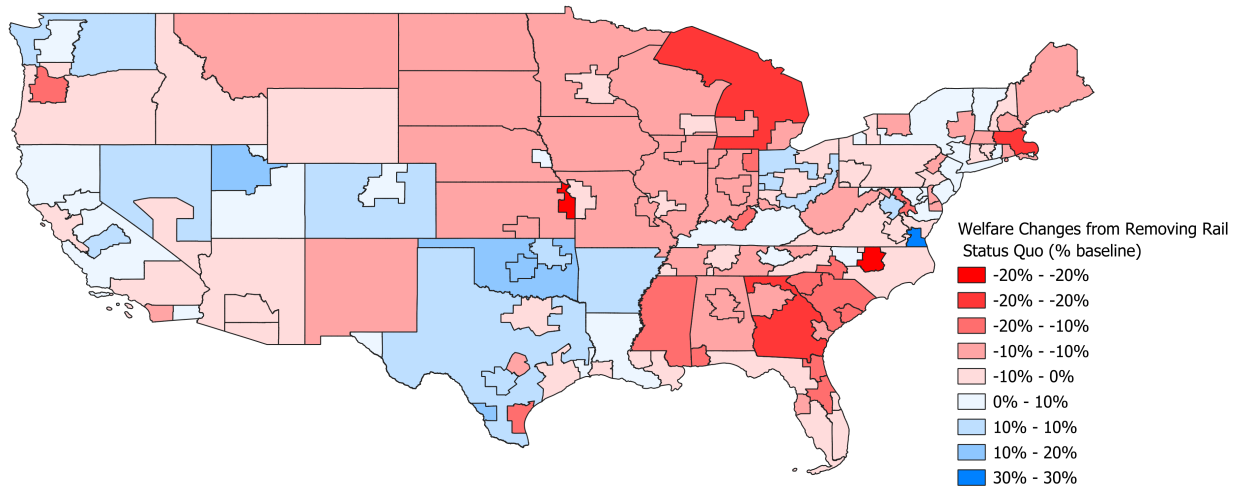
Table 6: Change in Real Exports under a Rail Strike

	Baseline Trade Share (%)	Subs. Effect (ppt)	Income Effect (ppt)	Total Change (ppt)
	(1)	(2)	(3)	(4)
A. Status-Quo Freight Pricing				
Road	67.03	15.83	-2.97	12.87
Rail	11.39	-11.39	0.00	-11.39
Water	8.20	0.71	-0.42	0.30
Air	6.33	1.89	-0.79	1.10
Multi	7.05	-7.05	0.00	-7.05
Total	100.00	0.00	-4.17	-4.17
B. Perfect Freight Market Competition				
Road	68.90	14.21	-0.35	13.86
Rail	9.56	-9.56	0.00	-9.56
Water	8.93	0.52	-0.29	0.22
Air	5.99	1.44	-0.58	0.86
Multi	6.61	-6.61	0.00	-6.61
Total	100.00	0.00	-1.23	-1.23

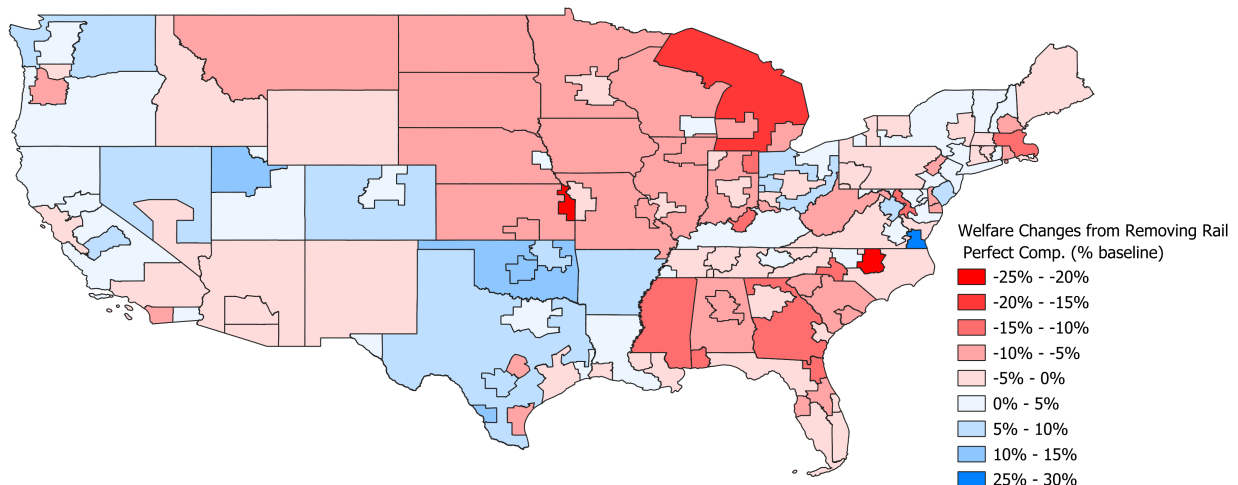
Notes: This table displays aggregate real export changes stemming from removal of rail and multi-modal transport. Column (1) displays each mode's share of national trade in baseline, and is included for reference; Column (2) lists the change in trade volumes across modes, holding incomes constant— note that, in this case, due to imperfect modal substitution and the elimination of certain modes, Column (2) need not sum to 0; Column (3) lists the change in trade volumes resulting from a change in income, holding mode, route, and port choices constant; Column (4) = Column (2) + Column (3) lists the total change in transport volume (as a percent of national welfare) along each mode. Panel A lists the change under status-quo freight pricing, while Panel B lists the change under perfect freight market competition. The simulated changes are calculated using 5 potential routings for each mode-origin-destination combination.

Figure 7: Geographic Welfare Incidence of a Rail Strike

(a) Status-Quo Freight Pricing



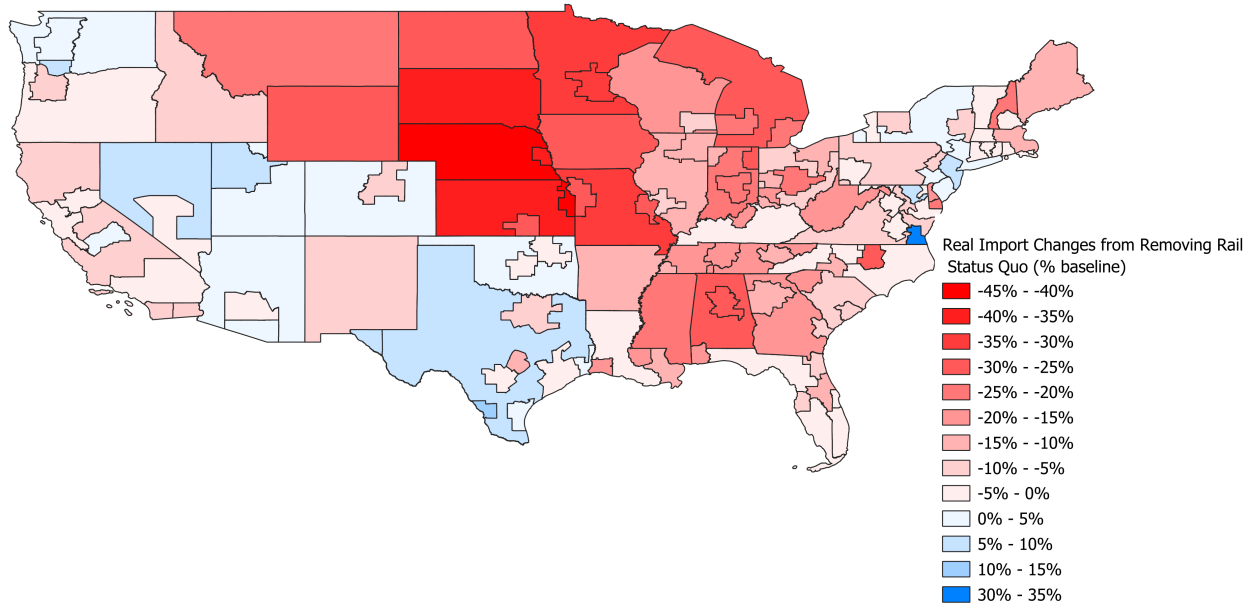
(b) Perfect Freight Market Competition



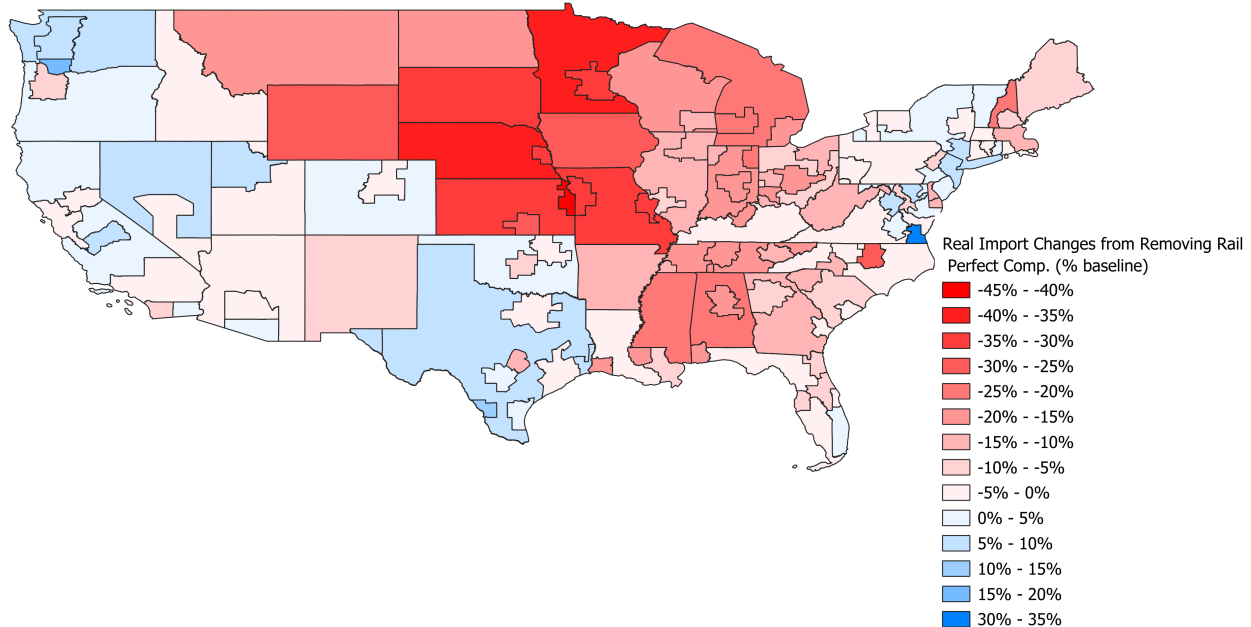
Notes: This figure presents percent changes in real welfare as a result of removing rail and multi-modal transport. Panel A reports welfare changes under the status-quo, while Panel B presents welfare changes under the perfect freight market competition. Darker colors signify greater changes—red denotes a decline in value, while blue denotes a gain.

Figure 8: Geographic Import Incidence of a Rail Strike

(a) Status-Quo Freight Pricing



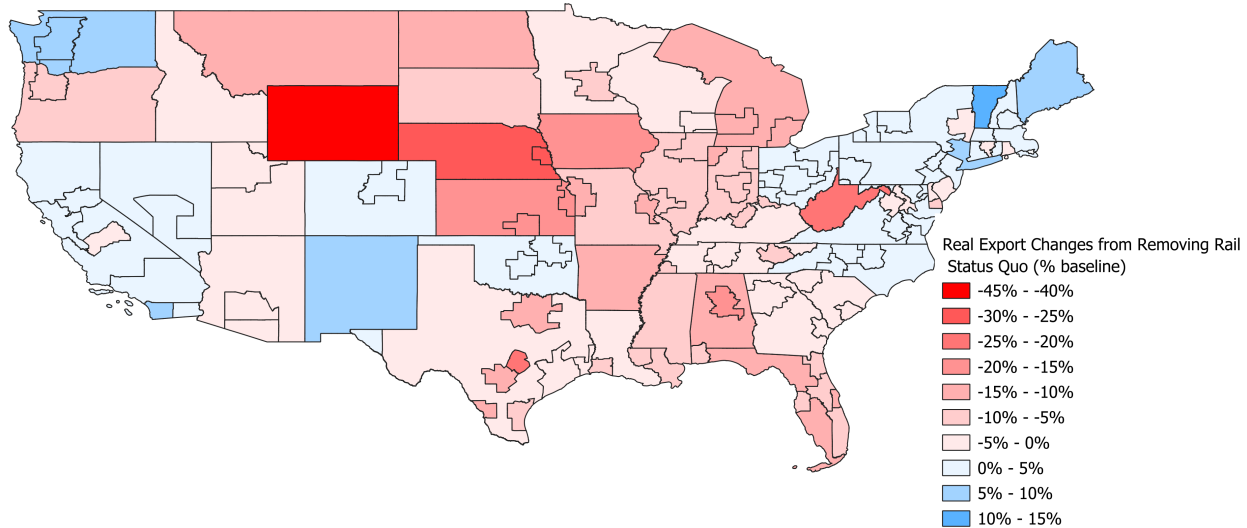
(b) Perfect Freight Market Competition



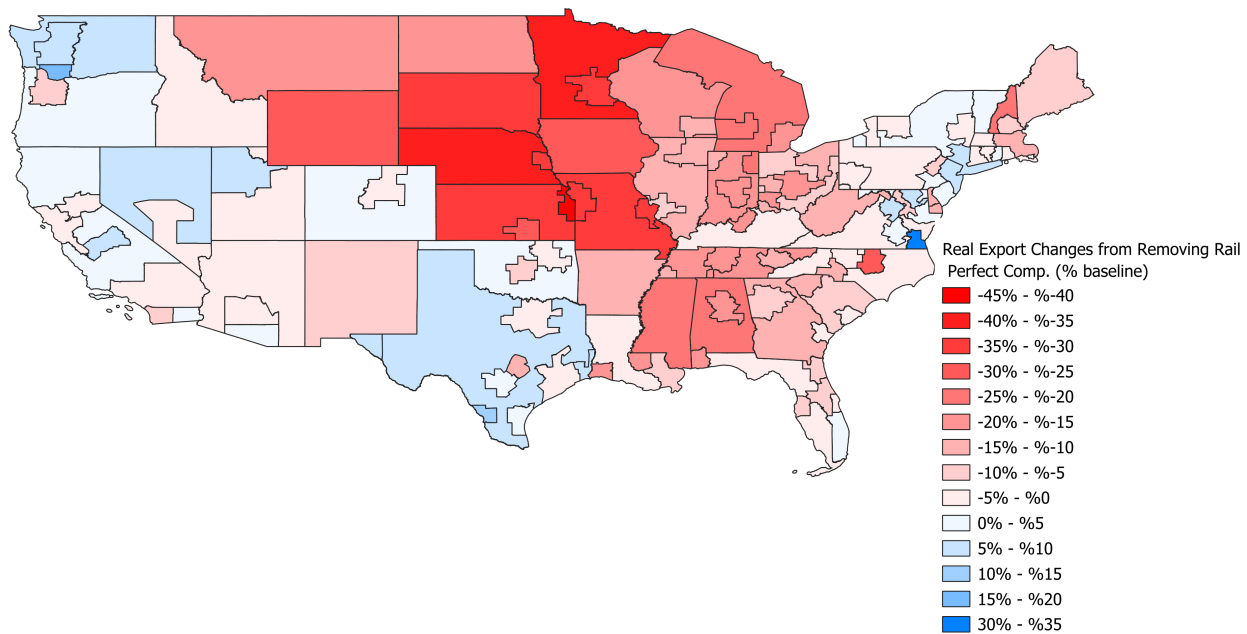
Notes: This figure presents percent changes in real imports as a result of removing rail and multi-modal transport. Panel A reports import changes under the status-quo, while Panel B presents import changes under the perfect freight market competition. Darker colors signify greater changes—red denotes a decline in value, while blue denotes a gain.

Figure 9: Geographic Export Incidence of a Rail Strike

(a) Status-Quo Freight Pricing



(b) Perfect Freight Market Competition



Notes: This figure presents percent changes in real exports as a result of removing rail and multi-modal transport. Panel A reports export changes under the status quo, while Panel B presents export changes under the perfect freight market competition. Darker colors signify greater changes—red denotes a decline in value, while blue denotes a gain.

Table 7: Change in Real Welfare from an International Trade Shock

	Baseline Trade Share (%)	Subs. Effect (ppt)	Income Effect (ppt)	Total Change (ppt)
	(1)	(2)	(3)	(4)
A. Status-Quo Freight Pricing				
Road	78.84	-0.02	-5.33	-5.35
Rail	3.79	0.03	-0.41	-0.38
Water	1.61	0.02	-0.13	-0.10
Air	1.95	0.18	-0.28	-0.09
Multi	13.82	-0.22	-0.97	-1.19
Total	100.00	0.00	-7.11	-7.11
B. Perfect Freight Market Competition				
Road	80.75	-0.05	-5.56	-5.61
Rail	3.57	0.04	-0.39	-0.35
Water	1.80	0.02	-0.13	-0.11
Air	1.81	0.22	-0.28	-0.05
Multi	12.07	-0.24	-0.87	-1.10
Total	100.00	0.00	-7.22	-7.22

Notes: This table displays national welfare changes stemming from an international trade shock meant to emulate the jump in prices sparked by the Covid-19 pandemic. Column (1) displays each mode's share of national trade in baseline, and is included for reference; Column (2) lists the change in trade volumes across modes, holding incomes constant; Column (3) lists the change in trade volumes resulting from a change in income, holding mode, route, and port choices constant; Column (4) = Column (2) + Column (3) lists the total change in transport volume (as a percent of national welfare) along each mode. The simulated changes are calculated using 5 potential routings for each mode-origin-destination combination.

Table 8: Change in Real Imports from an International Trade Shock

	Baseline Trade Share (%)	Subs. Effect (ppt)	Income Effect (ppt)	Total Change (ppt)
	(1)	(2)	(3)	(4)
A. Status-Quo Freight Pricing				
Road	60.72	-0.15	-10.55	-10.70
Rail	9.53	0.27	-1.87	-1.61
Water	3.35	0.17	-0.66	-0.49
Air	10.27	1.50	-2.04	-0.54
Multi	16.13	-1.79	-2.72	-4.51
Total	100.00	0.00	-17.84	-17.84
B. Perfect Freight Market Competition				
Road	64.46	-0.42	-11.08	-11.50
Rail	8.19	0.32	-1.63	-1.31
Water	3.02	0.19	-0.63	-0.44
Air	9.57	1.80	-2.02	-0.22
Multi	14.75	-1.89	-2.56	-4.46
Total	100.00	0.00	-17.92	-17.92

Notes: This table displays aggregate real import changes stemming from an international trade shock meant to emulate the jump in prices sparked by the Covid-19 pandemic. Column (1) displays each mode's share of national trade in baseline, and is included for reference; Column (2) lists the change in trade volumes across modes, holding incomes constant; Column (3) lists the change in trade volumes resulting from a change in income, holding mode, route, and port choices constant; Column (4) = Column (2) + Column (3) lists the total change in transport volume (as a percent of national welfare) along each mode. The simulated changes are calculated using 5 potential routings for each mode-origin-destination combination.

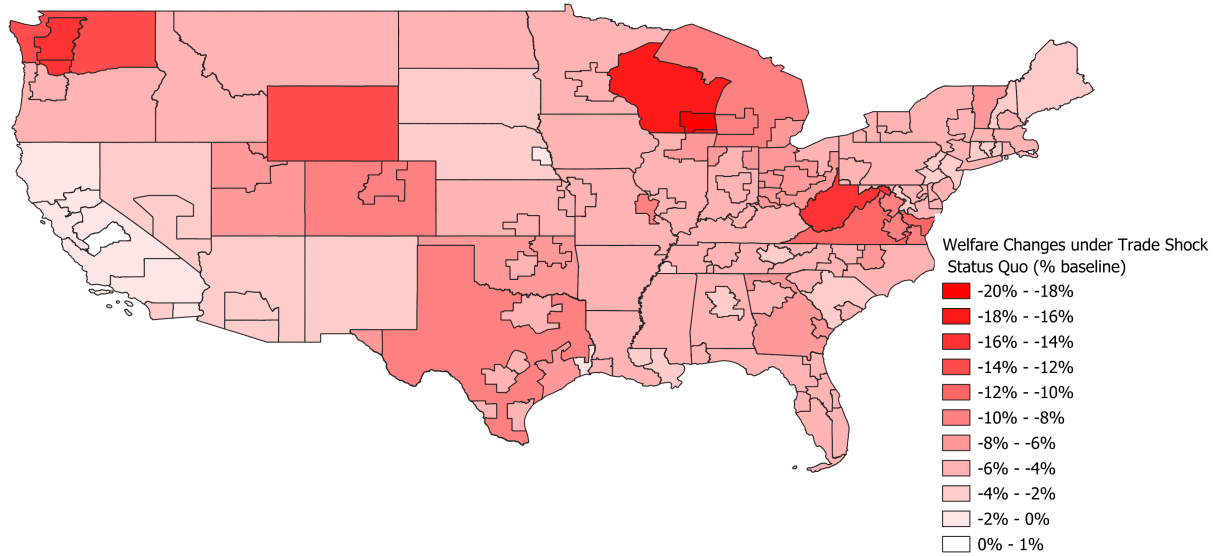
Table 9: Change in Real Exports from an International Trade Shock

	Baseline Trade Share (%)	Subs. Effect (ppt)	Income Effect (ppt)	Total Change (ppt)
	(1)	(2)	(3)	(4)
A. Status-Quo Freight Pricing				
Road	67.03	-0.73	-14.78	-15.52
Rail	11.39	0.00	-2.61	-2.61
Water	8.20	0.36	-2.04	-1.68
Air	6.33	-0.19	-1.50	-1.69
Multi	7.05	0.57	-1.74	-1.16
Total	100.00	0.00	-22.67	-22.67
B. Perfect Freight Market Competition				
Road	68.90	-0.87	-15.12	-15.99
Rail	9.56	0.17	-2.23	-2.06
Water	8.93	0.32	-2.19	-1.87
Air	5.99	-0.22	-1.42	-1.63
Multi	6.61	0.60	-1.64	-1.04
Total	100.00	0.00	-22.59	-22.59

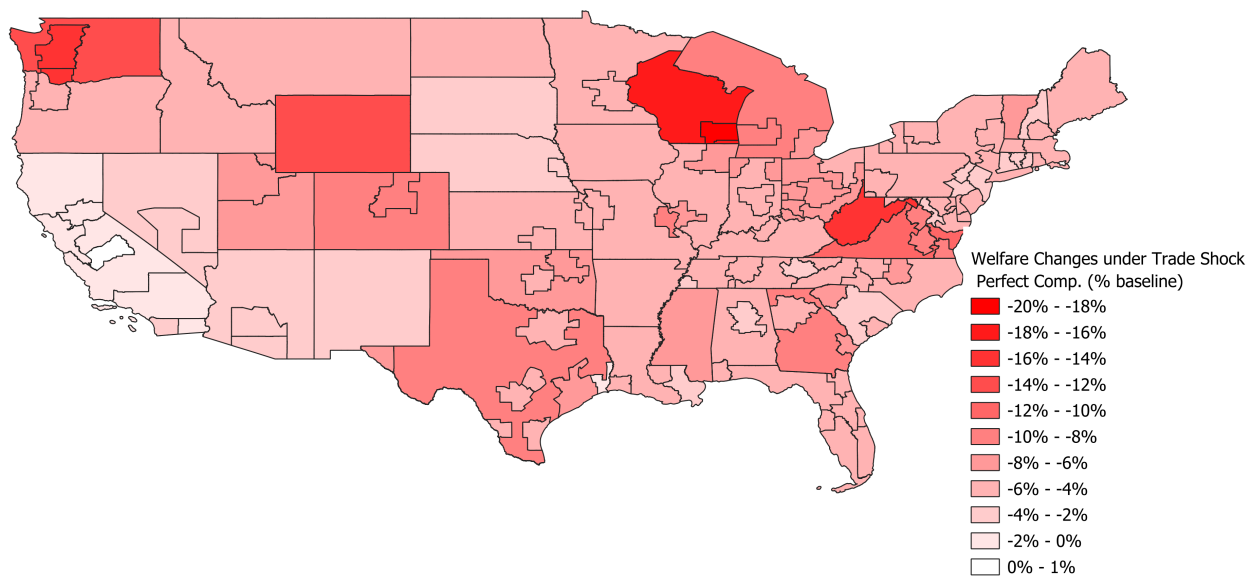
Notes: This table displays aggregate real export changes stemming from an international trade shock meant to emulate the jump in prices sparked by the Covid-19 pandemic. Column (1) displays each mode's share of national trade in baseline, and is included for reference; Column (2) lists the change in trade volumes across modes, holding incomes constant; Column (3) lists the change in trade volumes resulting from a change in income, holding mode, route, and port choices constant; Column (4) = Column (2) + Column (3) lists the total change in transport volume (as a percent of national welfare) along each mode. The simulated changes are calculated using 5 potential routings for each mode-origin-destination combination.

Figure 10: Geographic Welfare Incidence of an International Trade Shock

(a) Status-Quo Freight Pricing



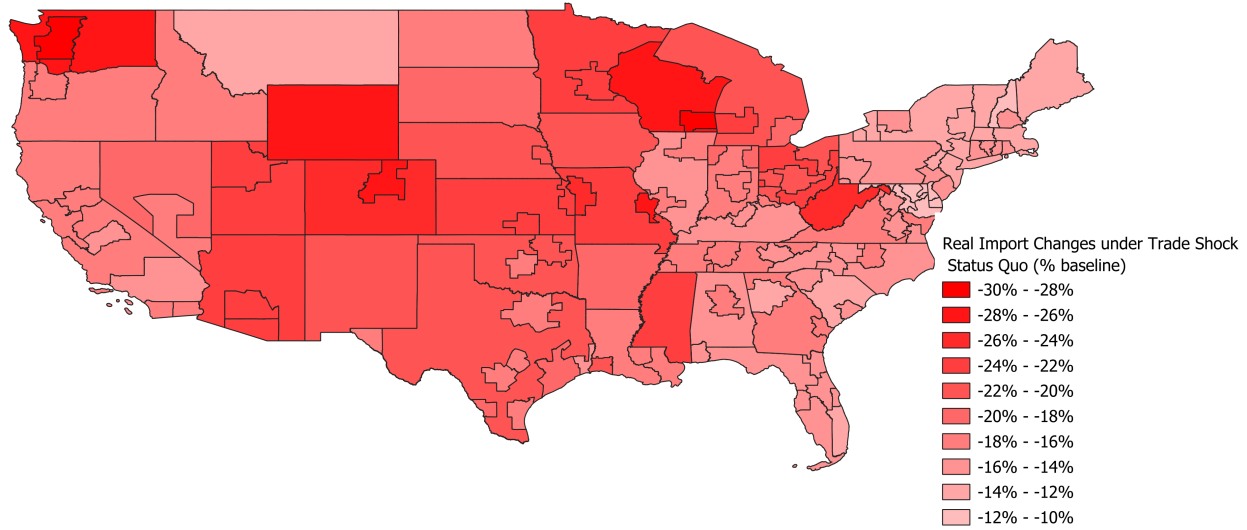
(b) Perfect Freight Market Competition



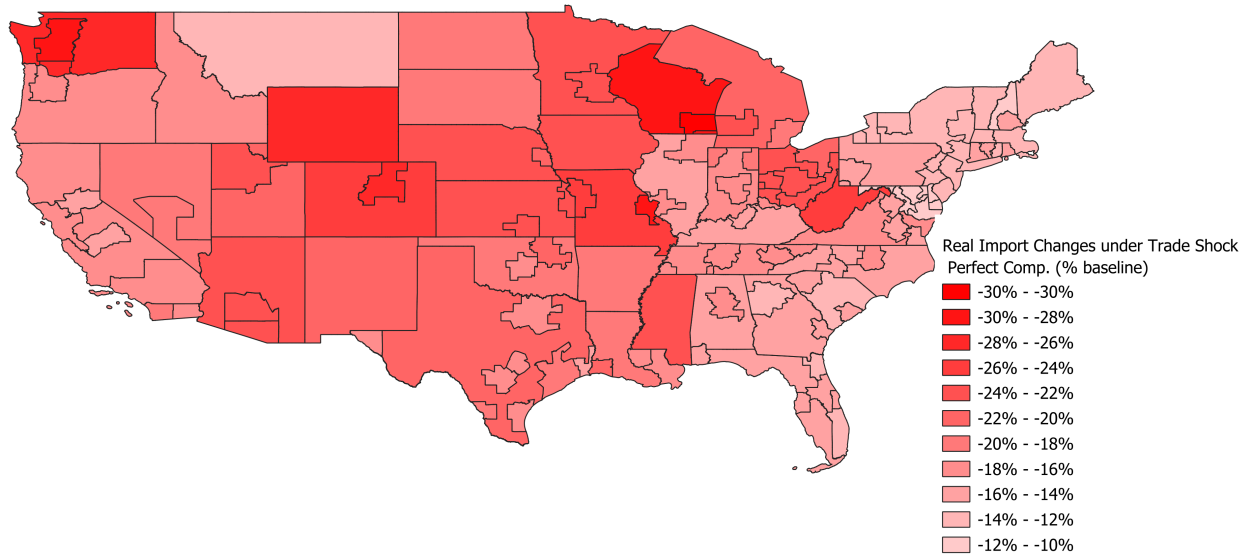
Notes: This figure presents percent changes in real welfare as a result of an international trade shock meant to emulate the spike in shipping prices witnessed during the Covid-19 pandemic. Panel A reports welfare changes under the status-quo, while Panel B presents welfare changes under the perfect freight market competition. Darker colors signify greater changes—red denotes a decline in value, while blue denotes a gain.

Figure 11: Geographic Import Incidence of an International Trade Shock

(a) Status-Quo Freight Pricing



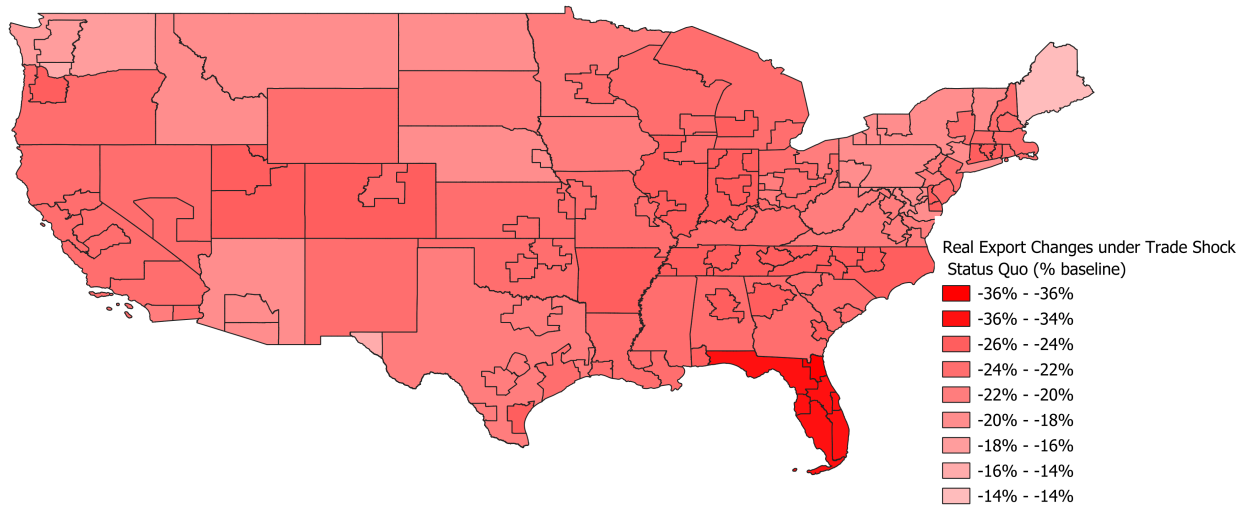
(b) Perfect Freight Market Competition



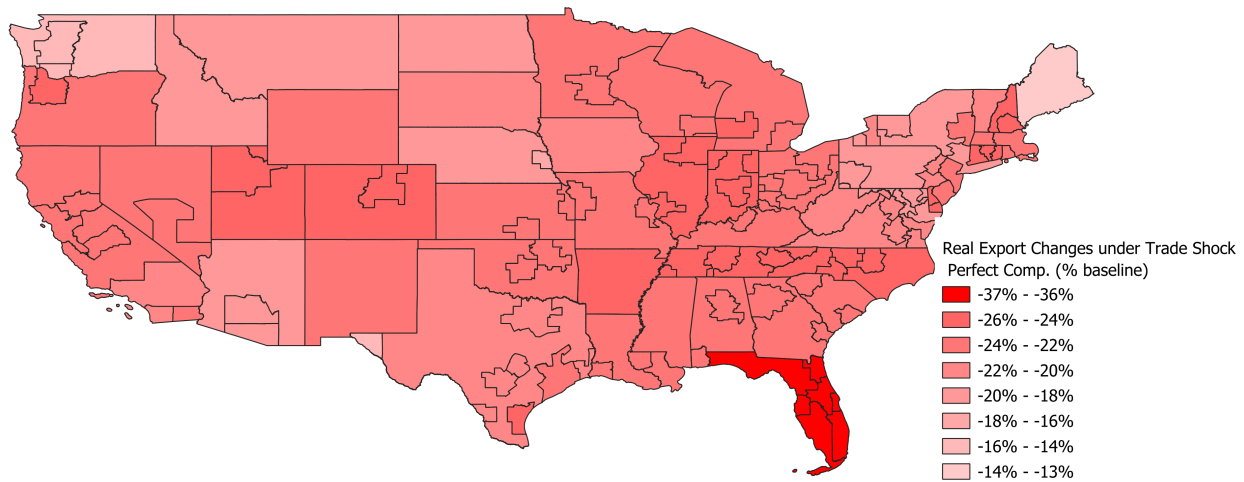
Notes: This figure presents percent changes in real imports as a result of an international trade shock meant to emulate the spike in shipping prices witnessed during the Covid-19 pandemic. Panel A reports import changes under the status-quo, while Panel B presents import changes under the perfect freight market competition. Darker colors signify greater changes—red denotes a decline in value, while blue denotes a gain.

Figure 12: Geographic Export Incidence of an International Trade Shock

(a) Status-Quo Freight Pricing



(b) Perfect Freight Market Competition



Notes: This figure presents percent changes in real exports as a result of an international trade shock meant to emulate the spike in shipping prices witnessed during the Covid-19 pandemic. Panel A reports export changes under the status-quo, while Panel B presents export changes under the perfect freight market competition. Darker colors signify greater changes—red denotes a decline in value, while blue denotes a gain.

A Mathematical Appendix

A.1 Simplifying Trade Shares

I begin with the trade shares from the nested logit structure:

$$\begin{aligned}\pi_{ir(e,x,m)|j} &= \pi_{r|iexmj} \pi_{m|iexmj} \pi_{ex|ij} \pi_{i|j} \\ &= \exp \left(-\ln A_i - \theta \left[\ln c_i + (\mu_{irj} + \kappa_r + u_{irj}) / (\varphi \rho \zeta) + (\alpha_{iem} + \gamma_{xmj}) / (\rho \zeta) + (\eta_{ie} + \nu_{xj}) / \zeta \right] \right. \\ &\quad \left. - (1 - \varphi) J_{iexmj} - (1 - \rho) V_{iexj} - (1 - \zeta) I_{ij} - Q_j \right).\end{aligned}$$

Unfortunately, this formulation is not a tenable regression specification. The inclusive values used to identify the correlation coefficients – J_{iexmj} , V_{iexj} , and I_{ij} – are not directly observed in the data; they could be calculated, though at substantial effort. Fixed effects do not offer a viable solution, as the origin-by-destination-by-mode fixed effect required to capture J_{iexmj} would absorb all of the non-simulated variation present in the data. However, some simple manipulation yields a much more tractable specification:

$$\begin{aligned}\ln \pi_{ir(e,x,m)|j} &= -\ln A_i - \theta \left[\ln c_i + (\mu_{irj} + \kappa_r + u_{irj}) / (\varphi \rho \zeta) + (\alpha_{iem} + \gamma_{xmj}) / (\rho \zeta) + (\eta_{ie} + \nu_{xj}) / \zeta \right] \\ &\quad + \theta [\eta_{ie} + \nu_{xj}] - \theta [\eta_{ie} + \nu_{xj}] + \rho \zeta V_{iexj} - \rho \zeta V_{iexj} \\ &\quad - (1 - \varphi) J_{iexmj} - (1 - \rho) V_{iexj} - (1 - \zeta) I_{ij} - Q_j \\ &= -\ln A_i - \theta \left[\ln c_i + (\mu_{irj} + \kappa_r + u_{irj}) / (\varphi \rho \zeta) + (\alpha_{iem} + \gamma_{xmj}) / (\rho \zeta) + \eta_{ie} + \nu_{xj} \right] \\ &\quad + (1 - \zeta) [-\theta(\eta_{ie} + \nu_{xj}) / \zeta + \rho V_{iexj} - I_{ij}] - (1 - \varphi) J_{iexmj} - (1 - \rho \zeta) V_{iexj} - Q_j \\ &= -\ln A_i - \theta \left[\ln c_i + (\mu_{irj} + \kappa_r + u_{irj}) / (\varphi \rho \zeta) + (\alpha_{iem} + \gamma_{xmj}) / (\rho \zeta) + \eta_{ie} + \nu_{xj} \right] \\ &\quad + (1 - \zeta) \ln \pi_{ex|ij} - (1 - \varphi) J_{iexmj} - (1 - \rho \zeta) V_{iexj} - Q_j \\ &= -\ln A_i - \theta \left[\ln c_i + (\mu_{irj} + \kappa_r + u_{irj}) / (\varphi \rho \zeta) + (\alpha_{iem} + \gamma_{xmj}) / (\rho \zeta) + \eta_{ie} + \nu_{xj} \right] \\ &\quad + \theta [\alpha_{iem} + \gamma_{xmj}] - \theta [\alpha_{iem} + \gamma_{xmj}] + \varphi \rho \zeta J_{iexmj} - \varphi \rho \zeta J_{iexmj} \\ &\quad + (1 - \zeta) \ln \pi_{ex|ij} - (1 - \varphi) J_{iexmj} - (1 - \rho \zeta) V_{iexj} - Q_j \\ &= -\ln A_i - \theta \left[\ln c_i + (\mu_{irj} + \kappa_r + u_{irj}) / (\varphi \rho \zeta) + \alpha_{iem} + \gamma_{xmj} + \eta_{ie} + \nu_{xj} \right] \\ &\quad + (1 - \rho \zeta) [-\theta(\alpha_{iem} + \gamma_{xmj}) / (\rho \zeta) + \varphi J_{iexmj} - V_{iexj}] \\ &\quad + (1 - \zeta) \ln \pi_{ex|ij} - (1 - \varphi \rho \zeta) J_{iexmj} - Q_j\end{aligned}$$

$$\begin{aligned}
&= -\ln A_i - \theta \left[\ln c_i + (\mu_{irj} + \kappa_r + u_{irj}) / (\varphi \rho \zeta) + \alpha_{iem} + \gamma_{xmj} + \eta_{ie} + \nu_{xj} \right] \\
&\quad + (1 - \rho \zeta) \ln \pi_{m|ie} + (1 - \zeta) \ln \pi_{ex|ij} - (1 - \varphi \rho \zeta) J_{ie} - Q_j \\
&= -\ln A_i - \theta \left[\ln c_i + (\mu_{irj} + \kappa_r + u_{irj}) / (\varphi \rho \zeta) + \alpha_{iem} + \gamma_{xmj} + \eta_{ie} + \nu_{xj} \right] \\
&\quad + \theta [\mu_{irj} + \kappa_r + u_{irj}] - \theta [\mu_{irj} + \kappa_r + u_{irj}] \\
&\quad + (1 - \rho \zeta) \ln \pi_{m|ie} + (1 - \zeta) \ln \pi_{ex|ij} - (1 - \varphi \rho \zeta) J_{ie} - Q_j \\
&= -\ln A_i - \theta \left[\ln c_i + \mu_{irj} + \kappa_r + u_{irj} + \alpha_{iem} + \gamma_{xmj} + \eta_{ie} + \nu_{xj} \right] \\
&\quad + (1 - \varphi \rho \zeta) [-\theta(\mu_{irj} + \kappa_r + u_{irj}) / (\varphi \rho \zeta) - J_{ie}] \\
&\quad + (1 - \rho \zeta) \ln \pi_{m|ie} + (1 - \zeta) \ln \pi_{ex|ij} - Q_j \\
&= -\ln A_i - \theta \left[\ln c_i + \mu_{irj} + \kappa_r + u_{irj} + \alpha_{iem} + \gamma_{xmj} + \eta_{ie} + \nu_{xj} \right] \\
&\quad + (1 - \varphi \rho \zeta) \ln \pi_{r|ie} + (1 - \rho \zeta) \ln \pi_{m|ie} + (1 - \zeta) \ln \pi_{ex|ij} - Q_j.
\end{aligned}$$

A.2 Price Index

I now provide a detailed derivation of Equation (14). Let $\mathbf{p}_j(\omega)^\top = [p_{irj_1}(\omega) \ p_{irj_2}(\omega) \ \dots]$ be the vector of prices for good ω in market j . Define similarly the vectors $\boldsymbol{\mu}_j$, $\boldsymbol{\tau}_j$, $\boldsymbol{\epsilon}_j(\omega)$, and \mathbf{c}_j . Let $\mathbf{z} \in \mathbb{R}_{++}^N$, where N is the number of unique trade routes serving j . Define the function:

$$\begin{aligned}
G_j(z) &= \Pr(\mathbf{p}_j(\omega) \leq z) \\
&= \Pr\left(\frac{\mathbf{c}_j \circ \boldsymbol{\tau}_j \circ \boldsymbol{\mu}_j}{\boldsymbol{\epsilon}_j(\omega)} \leq \mathbf{z}\right) \\
&= \Pr\left(\frac{\mathbf{c}_j \circ \boldsymbol{\tau}_j \circ \boldsymbol{\mu}_j}{\mathbf{z}} \leq \boldsymbol{\epsilon}_j(\omega)\right) \\
&= \Pr(\ln \mathbf{c}_j + \ln \boldsymbol{\tau}_j + \ln \boldsymbol{\mu}_j - \ln \mathbf{z} \leq \ln \boldsymbol{\epsilon}_j(\omega)) \\
&= 1 - \Pr(\ln \mathbf{c}_j + \ln \boldsymbol{\tau}_j + \ln \boldsymbol{\mu}_j - \ln \mathbf{z} \geq \ln \boldsymbol{\epsilon}_j(\omega)) \\
&= 1 - F_j(\ln \mathbf{c}_j + \ln \boldsymbol{\tau}_j + \ln \boldsymbol{\mu}_j - \ln \mathbf{z}) \\
&= 1 - \exp\left(-\sum_{i \in \mathcal{S}} \left(\sum_{e,x \in \mathcal{S}^d} \left(\sum_{m \in \mathcal{M}} \left(\sum_{r \in \mathcal{R}_{ex}^m} \exp\left(\frac{-\ln A_i - \theta(\ln c_i + \ln \tau_{irj} + \ln \mu_{irj} - \ln z)}{\varphi \rho \zeta}\right)\right)^\varphi\right)^\rho\right)^\zeta\right) \\
&= 1 - \exp\left(-z^\theta \sum_{i \in \mathcal{S}} \left(\sum_{e,x \in \mathcal{S}^d} \left(\sum_{m \in \mathcal{M}} \left(\sum_{r \in \mathcal{R}_{ex}^m} \exp\left(\frac{-\ln A_i - \theta(\ln c_i + \ln \tau_{irj} + \ln \mu_{irj})}{\varphi \rho \zeta}\right)\right)^\varphi\right)^\rho\right)^\zeta\right) \\
&= 1 - \exp(-z^\theta Q_j).
\end{aligned}$$

From the CES utility assumption, it follows,

$$\begin{aligned}
p_j &= \left(\int_{\Omega} p_j(\omega)^{1-\sigma} d\omega \right)^{\frac{1}{1-\sigma}} \\
p_j^{1-\sigma} &= \int_0^1 z^{1-\sigma} dG_j(z) \\
p_j^{1-\sigma} &= \int_{\mathbb{R}_{++}} z^{\theta-\sigma} \exp(-z^\theta Q_j) \theta Q_j dz \\
p_j^{1-\sigma} &= \Gamma\left(\frac{\theta+1-\sigma}{\theta}\right) Q_j^{\frac{\sigma-1}{\theta}} \\
p_j &= \Gamma\left(\frac{\theta+1-\sigma}{\theta}\right)^{\frac{1}{1-\sigma}} Q_j^{-\frac{1}{\theta}}.
\end{aligned}$$

A.3 Derivatives of trade shares

I begin with the derivative of the trade share along a route r with respect to its own markup:

$$\frac{\partial \pi_{ir|j}}{\partial \mu_{irj}} = - \left(\frac{\theta}{\varphi \rho \zeta} \right) \pi_{ir|j} (1 - (1 - \varphi) \pi_{r|iemj} - \varphi(1 - \rho) \pi_{rm|ieej} - \varphi \rho (1 - \zeta) \pi_{rem|ij} - \varphi \rho \zeta \pi_{ir|j}).$$

Now, I consider the derivatives of trade shares with respect to markups along competing routes. Let $m(r), x(r)$ denote the mode, port of entry/exit for a particular route r . If $r \neq r'$ but $m(r) = m(r')$ and $x(r) = x(r')$, then

$$\frac{\partial \pi_{ir|j}}{\partial \mu_{ir'j}} = \left(\frac{\theta}{\varphi \rho \zeta} \right) \pi_{ir|j} ((1 - \varphi) \pi_{r'|iemj} + \varphi(1 - \rho) \pi_{r'm|ieej} + \varphi \rho (1 - \zeta) \pi_{r'rem|ij} + \varphi \rho \zeta \pi_{ir'|j}).$$

If $r \neq r'$ and $m(r) \neq m(r')$ but $x(r) = x(r')$, then

$$\frac{\partial \pi_{ir|j}}{\partial \mu_{ir'j}} = \left(\frac{\theta}{\varphi \rho \zeta} \right) \pi_{ir|j} (\varphi(1 - \rho) \pi_{r'm|ieej} + \varphi \rho (1 - \zeta) \pi_{r'rem|ij} + \varphi \rho \zeta \pi_{ir'|j}).$$

If $r \neq r'$ and $m(r) \neq m(r')$ and $x(r) \neq x(r')$, then

$$\frac{\partial \pi_{ir|j}}{\partial \mu_{ir'j}} = \left(\frac{\theta}{\varphi \rho \zeta} \right) \pi_{ir|j} (\varphi \rho (1 - \zeta) \pi_{r'rem|ij} + \varphi \rho \zeta \pi_{ir'|j}).$$

If $i \neq i'$, then

$$\frac{\partial \pi_{ir|j}}{\partial \mu_{i'r'j}} = \theta \pi_{ir|j} \pi_{i'r'|j}.$$

Finally, it should be noted that I assume all destinations enjoy completely independent freight markets, such that, for all $j \neq j'$

$$\frac{\partial \pi_{ir|j}}{\partial \mu_{i'r'|j'}} = 0.$$

A.4 Proof of Convergence of the EM Algorithm

It will prove convenient to define the following matrices:

$$\begin{aligned}\boldsymbol{\phi}^\top &= \begin{bmatrix} \lambda_i & \beta_m & 1 - \zeta & 1 - \rho\zeta & 1 - \varphi\rho\zeta \end{bmatrix} \\ X_{irj} &= \begin{bmatrix} \delta_{irj} & Miles_{irj} \times \mathbb{1}(m) & \ln \pi_{ex|ij} & \ln \pi_{m|iexj} & \ln \pi_{r|iexmj} \end{bmatrix}\end{aligned}$$

where $\mathbb{1}$ denotes the indicator function. With these matrices, I re-define my primary estimating equation:

$$\ln \boldsymbol{\pi} = \mathbf{X}\boldsymbol{\phi} + \mathbf{u}. \quad (22)$$

where $\boldsymbol{\pi}^\top = [\pi_{ir_1|j} \ \pi_{ir_2|j} \ \dots]$, $\mathbf{X}^\top = [X_{ir_1j} \ X_{ir_2j} \ \dots]$, and $\mathbf{u}^\top = [u_{ir_1j} \ u_{ir_2j} \ \dots]$ denote the matrix representation of each variable. Obviously, Equation (22) presents the complete-information estimating equation. Unfortunately, elements of both \mathbf{X} and $\ln \boldsymbol{\pi}$ are unobserved.³⁷ I therefore rely on the incomplete-information formulation:

$$\ln \boldsymbol{\pi}^{(p)} = \mathbf{X}^{(p)}\boldsymbol{\phi} + \mathbf{u}, \quad (23)$$

where $\ln \boldsymbol{\pi}^{(p)} = \mathbb{E}(\ln \boldsymbol{\pi}|\boldsymbol{\phi}^{(p)})$ and $\mathbf{X}^{(p)} = \mathbb{E}(\mathbf{X}|\boldsymbol{\phi}^{(p)})$ denote the expected values of $\ln \boldsymbol{\pi}$ and \mathbf{X} for some, fixed value of $\boldsymbol{\phi}^{(p)}$. Estimating Equation (23) via OLS³⁸ yields the next entry in the EM sequence, $\boldsymbol{\phi}^{(p+1)}$; denote the residuals from this estimation $\mathbf{u}^{(p+1)} = \ln \boldsymbol{\pi}^{(p)} - \mathbf{X}^{(p)}\boldsymbol{\phi}^{(p+1)}$. From

³⁷Specifically, δ_{irj} and $\pi_{r|iexmj}$ are unobserved in my data.

³⁸Note that OLS estimation satisfies the criteria of the EM process, as OLS estimates are also maximum-likelihood estimates.

here, define the likelihood function:

$$Q(\phi^{(p+1)} | \phi^{(p)}) = \mathbb{E} \left[\ln f(\mathbf{X} | \phi^{(p+1)}) \middle| \phi^{(p)} \right]$$

where f is the probability of \mathbf{X} given ϕ . In words, $Q(\phi^{(p+1)} | \phi^{(p)})$ defines the log-likelihood of observing $\phi^{(p+1)}$ given $\phi^{(p)}$.

Per Wu (1983), a sufficient condition for convergence of the EM process is the existence of a forcing function $c > 0$ such that

$$Q(\phi^{(p+1)} | \phi^{(p)}) - Q(\phi^{(p)} | \phi^{(p)}) \geq c \|\phi^{(p+1)} - \phi^{(p)}\| \quad \forall p. \quad (24)$$

Note that this inequality holds trivially when $\phi^{(p+1)} = \phi^{(p)}$. I now focus on the case $\phi^{(p+1)} \neq \phi^{(p)}$. Given the assumption that $u_{irj} \sim N(0, v)$, it follows that

$$Q(\phi^{(p+1)} | \phi^{(p)}) = -(n/2) \ln(2\pi) - (n/2) \ln v - (1/(2v)) \mathbf{u}^{(p+1)\top} \mathbf{u}^{(p+1)}, \quad (25)$$

where n is the number of rows in \mathbf{X} . Note also that, thanks to the OLS estimation,

$$\phi^{(p+1)} = (\mathbf{X}^{(p)\top} \mathbf{X}^{(p)})^{-1} (\mathbf{X}^{(p)\top} \ln \boldsymbol{\pi}^{(p)}). \quad (26)$$

Combining equations (24) - (26) yields a characterization for c that satisfies Wu's criterion:

$$\frac{(\mathbf{u}^{(p+1)\top} \mathbf{u}^{(p+1)} - \mathbf{u}^{(p)\top} \mathbf{u}^{(p)})}{2v \left\| (\mathbf{X}^{(p)\top} \mathbf{X}^{(p)})^{-1} (\mathbf{X}^{(p)\top} \ln \boldsymbol{\pi}^{(p)}) - \phi^{(p)} \right\|} \geq c > 0. \quad (27)$$

The existence of c therefore hinges on three conditions: i) v must be non-zero and finite; ii) $\mathbf{X}^{(p)\top} \mathbf{X}^{(p)}$ must be invertible (in other words, \mathbf{X} must have non-zero variance); and iii) $\mathbf{X}^{(p)}$ and $\ln \boldsymbol{\pi}^{(p)}$ must have non-zero, finite covariance. That is, the same conditions required for OLS estimation guarantee convergence of the EM process.